COO-1233-23

Plasma Motion and Confinement in a Toroidal Octupole Magnetic Field*

R. A. Dory, D. W. Kerst, D. M. Meade,
W. E. Wilson & C. W. Erickson

Physics Department, University of Wisconsin, Madison, Wisconsin

Physics of Fluids

* Assisted in part by the U. S. Atomic Energy Commission

COO-1233-23

Plasma Motion and Confinement In A Toroidal Octupole Magnetic Field*

R. A. Dory**, D. W. Kerst, D. M. Meade,
W. E. Wilson‡, & C. W. Erickson

Physics Department, University of Wisconsin, Madison, Wisconsin

ABSTRACT

Plasma of approximately 100 electron volts ion energy was injected into and trapped within an octupole magnetic field with closed lines of force contained within a region of magnetohydrodynamic stability. A zero field locus was near the middle of the region, and fields of 1,000 gauss to 8,000 gauss existed along the wall and around the current carrying hoops forming the multipole field. Most of the experiments were made with 4.7 to 9.6 gyroradii across the stable plasma region. Plasma injected from the outside penetrated the magnetic field transversely

---

* Assisted in part by the U. S. Atomic Energy Commission.

** Present address: Oak Ridge National Laboratory, Oak Ridge, Tennessee.

‡ Present address: Battelle Northwest Laboratory, Richland, Washington.

by $\vec{E} \times \vec{B}$ drift caused by a transient polarization electric field. The self short circuit current on the looping contained lines of force was detected and measured as it stopped and trapped the plasma cloud. Flow of plasma followed the low field region around the toroid rapidly with the ion speed and generated an octupole electric field during filling. Fluctuating electric fields ejected some plasma to the wall, and there were evidences of inward instability when there were density voids near the center. $\vec{E} \times \vec{B}$ flow velocities and plasma densities were determined throughout the volume with electrostatic probes. Probes and microwave observations showed that the electron component had 10 eV temperature and remained the 2.5 milliseconds that the magnetic field continued with no sudden or catastrophic loss such as would accompany instability. The hot ions were extracted from the plasma interior by a field-free iron pipe for times of the order of a millisecond also with no catastrophic sudden losses. The observed mean life for the exponential decay of 100 volt ions was 0.4 milliseconds which agrees with calculated loss on probes and hoop supports. Ions of other energies had lifetimes proportional to the reciprocal of their velocities. Densities at

the injection region were 10^{12} per cm^3, and after spreading throughout the confining region, the density was $\sim 10^9$ per cm^3 with more than 10% trapping efficiency.

After 100 microseconds, the large electric fields present during filling died away the plasma apparently acquired a boundary with small electric potential differences compared to the 100 eV energies of contained ions. This quiescent condition continued while the plasma was gradually being lost on probes and supports.

I. Introduction

The idea of containing a hot plasma in a multipole or "cusped" magnetic field has early origins,[1] and it now has a revived interest in the form of the study of "Minimum B" configurations. In spite of the attraction of magnetohydrodynamic stability expected from the increase of field strength with outward displacement, the plasma leak along escaping lines of force has been a major disadvantage to the containment of plasma in "cusped" systems. In the original cusp, the leak is large and it increases with temperature. S. I. Braginskii and B. B. Kadomtsev[2] pointed out the possibility of having a multipole field region with all its lines of force confined within the vacuum chamber by current carrying conductors so that lines of force do not escape to the walls, as in the original cusp, but rather so that they return to the multipole field region by passing around the current carrying rods. Thus the plasma would not be lost by following lines of force, and net magnetohydrodynamic stability could still be maintained. Several structures for accomplishing this were pointed out by J. L. Tuck,[3] and the value of such systems was brought up and emphasized by him.

These suggestions make use of the fact that magnetic lines are continuous and the plasma leak can be closed by allowing the lines to come back into the cusp region (Figure); however, where lines are brought back, the curvature of the lines is such that they do not bulge into the plasma. Then outward plasma displacements would be toward weaker fields and stability would not be contributed by such a region. These are the regions where lines of force pass around the current carrying rods--the "bridge" regions of Tuck. As Figure shows, lines of force outside the $\psi = 0$ separatrix are alternately convex toward the plasma and concave toward the plasma. The net effect can be stability if the communication along the line of force is sufficient to cause the tube of flux to act as a whole in flute production. However, far out from the rods, there is a limiting critical flux line, ψ_c, beyond which there is no interchange stability since the volume of a tube of unit flux increases. Earlier considerations of stability gave various ways of looking at this problem,[2,4] but for a real case to be constructed, the field pattern must be well known, and digital computer methods have proved necessary for finding the most useful shapes of conducting rods and walls and for finding ψ_c.

The experiments described here use equipment of the minimum size that seems capable of giving useful experience and interesting plasma results in the study of multipoles. However, one can hardly expect to fill such a multipole (10^5 cc.) to its stability limit[4] with existing guns even with perfect trapping efficiency since they would provide orders of magnitude too little 100 ev plasma. The size chosen was sufficient for about eight 100 ev proton gyroradii across the stable region, and the vacuum problem was greatly simplified by choosing this ion energy so that the charge exchange cross section is very low in molecular hydrogen. Hydrogen lifetimes for charge exchange plasma loss can be much greater than 10^{-3} seconds for easily attained vacuua of 10^{-6} to 10^{-7} torr. of molecular hydrogen. Even in the pessimistic case of background atomic hydrogen gas where, from zero to 80 kev., $\tau_{ex} = 10^7/n_v$ sec., a density of atomic hydrogen $n_v \sim 10^{10}$, which is near 10^{-7} torr., would give the lifetime for charge exchange of 10^{-3} sec.

The structure contains closed current-carrying hoops near the interior corners of an approximately square conducting toroidal vacuum box. These hoops must either be levitated magnetically by shaping the box corners and by inducing current in

the hoops, or they may have small mechanical supports.[5] Current can be brought to the hoop from the outside by the conductor pairs which support the hoops. Three narrow supports on each of the four hoops were used in this experiment, and the current was induced in them by a transformer core carrying magnetic flux through the center of the toroidal vacuum box.

The goal was to limit the unavoidable losses of plasma due to charge exchange plus loss on supports so that plasma lifetime from all such causes would be 10^{-3} seconds or greater. This requires that the magnetic field pulse be maintained for several milliseconds. A pulse length of .005 seconds for a half sine wave was used. In the time of the pulse, the magnetic field diffuses into the conducting hoops and walls. This diffusion should be slow enough to maintain a useful field pattern for the duration of the experiment, and hoop hangers must be small enough so that they do not annihilate plasma following lines of force too quickly. A rough estimate of the lifetime due to loss on supports can be made as follows:

$$\tau = V/(A_{\perp} v_{\parallel})$$

where V is the plasma volume, $A_{\perp}$ the area of the support perpendicular to the field lines, and $v_{\parallel}$ is the average velocity of the ions along the field lines.

The supports are .15 cm. thick by 1 cm. wide, three to a hoop on four hoops. To be conservative, the area should include two ion gyroradii in its width. The length of the support between the outer rods and the critical ψ line is 2.8 cm. or 8.2 gyroradii plasma width for 100 ev hydrogen ions. Many runs were made at lower fields with 4.7 gyroradii plasma width. At the low field amplitude with 100 ev ions spiraling at 45°, there are $4.7\sqrt{2}$ gyroradii and an effective velocity of $(1.5/\sqrt{2}) \times 10^7$ cm./sec. Thus $\tau = \frac{170 \times 10^3 \text{ cm.}^3 \times 2}{4 \times 3 \times 2.8 \times 1.35 \times 1.5 \times 10^7} = 0.5 \times 10^{-3}$ seconds. At the higher fields, 100 volt ions would survive longer. Also in the pessimistic case of an isotropic ion flux to the hangers, the lifetime is 0.5×10^{-3} seconds. The ion plasma component is collisionless in the time of the experiment so the lifetime is not limited by plasma diffusion.

Since the lines of force are all contained in the plasma confinement region, it is necessary either to form the plasma within the region somehow, or to inject plasma across lines of force. For this experiment, plasma from a gun giving a spectrum of ions in the 100 volt region passed through a differential pumping chamber to trap gas from the gun, then through slots

in a wall opening with area 5 cm. x 5 cm. The slots were circumferential allowing wall currents to flow so that the wall opening would not perturb the multipole field shape greatly. The collimated ion motion, produced by the 150 cm. flight from gun to multipole, Figure [2], provides a plasma cloud in which approximately unidirectional ions hold together the coincident electron cloud. The plasma need not create a large diamagnetic current around its perimeter where it enters a magnetic field. The small displacement current created at the entering surface of the cloud is sufficient to make a polarization field which allows the following and the interior ions to continue on straight paths. Thus the plasma and the field penetrate each other. The detailed descriptions of the densities and the motion of the plasma cloud and its fragments determined by $\vec{v}/c = \vec{E} \times \vec{B}/B^2$ at the injection port and at all points in the toroid where plasma flows during filling are some of the main results of this experiment.[6,7]

Excitation of the octupole generates some electric fields which have an influence on plasma motion. First there is the necessary split in the conducting toroid wall which encircles the exciting transformer core. At peak magnetic field, there

is no dI/dt, and hence no voltage across this gap except for the losses or IR voltage drop in the wall. Thus injection at or near peak field eliminates the large part of the gap electric field which would influence plasma motion. On the rising part of the field wave, the wattless gap electric field would push plasma circumferentially away from the gap, and on the falling part of the field, the plasma, which has been injected, would move into the gap by $\vec{E} \times \vec{B}$ drifts. The strategy is to use a slowly rising and falling magnetic field so the gap voltage is small (about 40 volts peak in this experiment), and to thereby obtain a sufficiently deep penetration of currents into the wall so that skin resistance, and thus wall IR voltage drop, is low. If the wall skin resistance is low, the tangential electric field is low, and it is this tangential electric field which drives plasma into the wall. In other words, a low resistance skin produces a very slow diffusion of the flux plot into the surface, and thus the plasma which follows the diffusing field lines is swept very slowly into the wall. In this experiment, the total wall voltage drop has been kept down to approximately 7 volts. This is less than the ionization potential, and the

$\vec{cE} \times \vec{B}/B^2$ drift velocity into the wall, which it generates, is $\sim$ 200 cm./sec. Thus in a millisecond, the flux plot and the plasma would only move a couple of millimeters into the wall or rods.

It is possible to program the wall current as a function of time so that the surface electric field can be zero or even reversed for short periods of time near peak field. Such programs have been tested by D. Baker at Los Alamos.[8] Normally, by the time the field has been brought back to zero after the pulse, all the plasma has been carried by the lines of force out the gap or into the wall.

Diagnostic techniques, which were available, were determined largely by the densities used for this experiment. Near the injection region, $n \cong 10^{12}$ per cm.^{3}, and later when the plasma was distributed around the confining region, typical densities were generally 10^9. This made the Langmuir probe and other electrostatic probes especially suitable for obtaining a wide variety of data.[6] In fact, four phenomena were immediately conspicuous with such probes. First, the plasma stream generates a polarization electric field at the injection region which gives

it an $\vec{E} \times \vec{B}$ drift toward the zero field locus in the multipole. The observed diamagnetic displacement of field lines is not sufficient or necessary for inward motion even with the most intense collimated plasma streams.[9] Second, the plasma flows around the toroid near the zero field locus crossing field lines as it flows with the same transit speed at which it traveled in field-free flight from the gun to the injection port in the multipole wall. Third, large electric fields accompany this field crossing and give the right $\vec{E} \times \vec{B}$ drift velocity showing that the motion during filling is dominated by this drift and that a good speed detector for the plasma velocity perpendicular to the magnetic field is such electrostatic probe. Fourth, the density of the clouds can be followed in space and time with such probes using the saturated ion current as a measure.

In addition to electrostatic probes, magnetic probes in the form of coils and Rogowski loops (current transformers) could be used with amplification at these densities. Currents and magnetic fields accompanying the depolarization and trapping of plasma and the bending of plasma around the toroid were determined with such coils.

One other useful probe was a combination electrostatic ion energy analyzer [10, 17] and a small diameter long tube of magnetic shielding material to extract hot ions out of the plasma. The tube was inserted into the center of the confining region to bring the ions through the multipole field to the external energy analyzer. This equipment gave observations of the time dependence of the densities of ions of any energy for different positions in the plasma. The iron pipe was inserted along a plane of constant scalar magnetic potential to minimize the distortion of the magnetic field.

Three cm. electromagnetic waves were used to determine the total number of electrons in the conducting vacuum box which acts like a multi-mode resonant cavity. The shift of the resonant frequencies is proportional to the average plasma density in the cavity.[7]

All these diagnostic devices showed only gradual disappearance of electron and ion components of the plasma as the magnetic field decreased or as plasma was lost on probes or hangers. Only during the filling time were bursts of plasma loss seen. Also during filling, occasionally the density gradient became

inverted compared to the stable density distribution (for example, the density at the zero field locus should be maximum; sometimes there was a transient minimum). Immediately radio-frequency electric fields were generated as the density redistributed itself. Quite different diagnostic methods are used in a related experiment being carried out by Ohkawa and his associates.[18]

II. The Field Configuration and Absolute Containment

Four straight unidirectional currents of the same magnitude at the corners of a square in free space will make a linear octupole field about the zero field locus with the B lines closing around the rods. There would be a single field minimum, and a vacuum tank wall carrying the return current can be coincident with one of the field lines which encloses all four currents without distorting the field shape. For the endless, or toroidal, case, the four currents are not the same, and the zero field locus generally splits into three minima if the hoop currents are not correctly adjusted. These cases, the linear and the toroidal, in free space can be plotted by conformal mapping or by tabulated functions respectively. Either case can be excited to give the correct rod currents by induction (in a

small skin depth approximation) if the wall carrying the return current coincides with a free space field line, and if the rod surfaces coincide with the free space field lines--provided there is the same total flux linkage around each rod surface.

Construction is difficult and expensive if it must conform to the free space plot. In addition, the toroidal plots are distorted and the fields around the outer rods or hoops are far weaker than the fields around the inner hoops.[11] A minimum ratio of major diameter to minor diameter of the toroid is desirable to minimize the size of the apparatus; but for shapes one might hope to use, the magnetic pressure on the inner hoops might be as much as an order of magnitude greater than the magnetic pressure on the outer hoops for the free space flux plot. To simplify construction and to make the magnetic forces similar on the outer and inner hoops, the problem was cast in the form of a boundary value problem. A simple square minor cross section was adopted for the toroid and this is a flux, or ψ, surface. The closed hoop surfaces are likewise constant ψ surfaces, and with inductive excitation, they all automatically link the same total flux. Thus separate rod surfaces are also all at the

same ψ. The differential equation satisfied by ψ is

$$\left\{ \partial^2/\partial R^2 - (1/R)\ \partial/\partial R + \partial^2/\partial Z^2 \right\} \psi = 0,$$

which is not quite the Laplacian, but which can be solved by relaxation methods.

Figure 3 shows several cases of digital computer flux plots made for (a) toroidal rectangular cross section, (b) the same with corners cut off, (c) the same with corners cut off and walls brought in. The critical, ψ_c, line of the outer limit of stability is indicated on the plots for zero plasma pressure. It was determined by the computer which calculated the volume of equal flux tubes. The minimum volume occurs at ψ_c, Figure 4. The program used was Dory's "TORMESH".

These plots are the final results of several trials for different relative sizes and positions of inner and outer hoops. The trials with changes were necessary to form the degenerate single zero field locus which has a tendency to split. The inner hoops were moved farther from their corners than the outer hoops to make the fields passing around the rods comparable and to make the forces on inner and outer hoops similar. The computer program gives these forces. Figure 3d shows a linear octupole

for comparison with the toroidal cases of 35.8 cm. square box width and 50.8 cm. inner box diameter. The figure shows that with this fat toroid having a small ratio of major diameter to minor diameter there is very little distortion in the flux plot due to the radius of curvature. The free space four hoop plot would be very distorted. Figure 5 shows the field magnitudes as a function of position along the vertical central line through the vacuum box and along the median plane.

The box cross section adopted is shown in Figure 3b. Although 80% of the flux is stable in contrast to 90% for Figure 3c, construction was much simpler with the choice of 3b. The improvement of 3b over 3a, which has 70% stable flux, was sufficient to warrant simple filling of the corners with conducting material.

It is possible to construct the conducting walls with pockets in which the current carrying rods are magnetically suspended. This can eliminate the plasma loss on the supports. For a pulsed magnetic field, the supports would be withdrawn after the magnetic field has reached its peak and before the plasma is injected. A few computer experiments were made to study these configurations.

The planar quadrupole case, a cross section of which is shown in Figure 1a, is especially interesting. It consists of two hoops in the median plane, and hence the magnetic forces provide only compression. The design of this type of multipole has been extensively examined at the Los Alamos Laboratory.

All these configurations have a zero field minimum, but the influence of a uniform added B_z, such as a stellarator has, should be pointed out. To avoid toroidal effects consider a linear multipole. The curve of unit flux tube volume, $dV/d\Psi$, would be like that shown in Figure 4 where the volume is the volume within a flux surface, Ψ = constant. However, if a uniform field B_z, is superimposed along the length of the structure, we must take equal area cross sections in the plane perpendicular to B_z for equal quantities of flux. Thus unit flux has the same volume for all flux tubes. The addition of B_z thus destroys the strong $V'' \leq 0$ which gives interchange stability to multipole systems without B_z. We have instead $V''=0$ or there is no change in the volume of unit flux and this would imply neutral stability. The only inhibition to the interchange would be topological entanglement or shear. Attempts [12] are being made to restore some interchange stability over a useful volume to such stellarator-like structures with B_z. The rotational transform of the stellarator would keep the lines of force contained without their passing around

the multipole conductors which produce the minimum B. Then the multipole conductors would not be imbedded in plasma and they would be accessable which is a technical advantage. In addition the existence of B_z eliminates the zero B locus of a pure multipole and makes possible the adiabatic invariant orbital magnetic moment. Without B_z the magnetic moments of orbits change on passing near the zero field region. However, it should be remembered that for a multipole with no B_z the magnetic moment is constant all around the plasma edge since the peak plasma density is at the zero field point and the plasma edge is in a high field everywhere. In addition there are zones of absolute containment in the multipole without B_z because of another invariant, P_θ = constant.[13]

Writing the Hamiltonian for a particle in the toroidal case:

$H = (1/2m)\ (P_r^2 + P_z^2 + [P_\theta/r - (e/c)\ A]^2) + e\phi\ (r,z) = P^2/2m.$

This is a constant and so also is $P_\theta = mr^2\ \dot{\theta} + (e/c)\ Ar$ constant for the axially symmetric case with $\vec{A}$ in the θ direction but with $\vec{A}$ and ϕ independent of θ. Thus

$P^2 - 2me\phi\ (r,z) \geq [P_\theta/r - e/c\ A]^2$ since $\psi = \int_\theta \vec{A} \cdot \vec{ds}$, $\psi = 2\pi rA$.

This gives, for $\phi = 0$, $(e/2\pi c)\psi = P_\theta \pm rP$ (1)

as the zone of absolute containment in terms of ψ for an orbit with any chosen P_θ and P. The total flux within a given zone is proportional to r; that is, an absolute confinement zone does

not coincide with ψ lines in the toroidal case. (In the linear case, the absolute containment zones do coincide with ψ lines).

If we have a sufficient number of gyroradii across the plasma region, then the outer absolute containment zones do not contain small values of B, and the plasma is thus surrounded by regions where there is an adiabatic invariant, μ = magnetic moment, even though some θ dependent electric field might develop to destroy the constancy of P_θ. The libration limits of a particular particle orbit with μ = constant can be obtained if $P_\perp$ (r) and $\mathcal{I}$ are used in 1) instead of just P. Figure 6 shows the absolute containment zones, two of which do not contain the zero B region, but which come between the zero B region and the external walls.

The question of how particles can ever get into an absolute containment zone when they come from outside will be discussed in the sections on injection and transit.

III. Structure

Although a planar quadrupole consisting of two hoops, which have no net magnetic forces to move them (Figure 1a), has many constructional advantages, the octupole had a bigger volume at

low field and seemed to be easy to construct for a modest experiment. A square box, with a small major radius and with only the box corners cut off was simple and easy to build rapidly.

Hoops were 1 3/4 inch and 2 inch diameter hard copper bar rolled into circles and welded. The hangers to hold the hoops were beryllium copper properly heat treated to reach 200,000 psi tensile strength. Three hangers 0.15 centimeters thick and 1.0 centimeter wide support each hoop. The forces were determined by the computer in the course of solving the boundary value problem. The hangers are shock mounted on "Viton A" cushions. These cushions are in vacuum chambers attached outside the vacuum box through which a hanger continuation passes. Viton is especially suitable within the vacuum chamber. The recoil buckling is more dangerous than the initial tension for breaking thin hangers, therefore the Viton cushions for the initial power

stroke were 0.3 cm thick and 5 cm in diameter, while for the recoil stroke, they were 1.45 cm thick and the same diameter. Viton saturates or increases its stiffness greatly if it is compressed more than 30%.

A useful property of Viton made its choice especially suitable for a cushion in vacuum. It was found that about 90% of the energy of compression is absorbed if saturation does not occur. This helps greatly in minimizing recoil.

The vacuum seals between the lid of the toroid and the box were continuous Viton "O" rings. The azimuthal insulated slit of 0.075 cm in this lid and in the box, where the voltage is established by the iron core, have Viton strip gaskets which end butting against the circular lid gaskets. This pressing connection between Viton gaskets has been trouble-free, and it provided the solution to a difficult topological sealing problem.

Plasma was generated in a simple conical Z pinch gun.[14] The spectrum of hydrogen ion energy from this gun is shown in Figure 7. The plasma cloud travels 150. cm to the zero field point in the multipole, Figure 2. This flight distance through a differential pumping chamber eliminates a rush of neutral gas from the gun. The pressure in the multipole before injection is $\sim$3 to 6 x 10^{-7} torr. It takes about 350 microseconds before room temperature gas from the gun expanding into vacuum would reach the multipole in sufficient quantity to raise the background gas pressure in the multipole by 10^{-7} torr. To prevent this collimated gas from entering the confining region, a fast mechanical shutter capable of shutting in 200 microseconds was constructed.[15] Its rotating vanes, when open, are in line with the bars between the slots in the multipole wall so that they intercept no additional plasma. An electrical impulse rotates these vanes which stay shut for $\sim 10^{-3}$ seconds.

The sequence of events during one pulse is -- first, the triggering of the ignitrons which discharge 3,000 microfarads charged as high as 3,500 volts into the 0.8 x 10^{-3} henry

primary winding on the iron core of the octupole. Second, the gas valve which admits hydrogen into the gun is electrically opened near the peak field of the 100 cycle per second half oscillation of the multipole field. Third, if the gas shutter is used, it is triggered about 100 microseconds after the gas valve. Fourth, about 175 microseconds after the gas valve trigger, the ignitron discharges 9 microfarads of low inductance capacitors charged to 18 kilovolts through the plasma gun. A damping resistor of 0.1 ohms limits the gun to one discharge of 4 microseconds duration.

IV. Theory and Observations of the Injection Process

Since it has been shown in (1) that there are zones of absolute containment for particles provided all magnetic and electric fields in the plasma have no dependence on θ, we cannot take particles out of or put them into such zones unless we cause a θ dependence of a field during injection and later remove it, or unless we create charged particles with the proper P_θ within the zones. In this experiment, a plasma cloud is injected through the multipole field, from the outside, where the lines of force are concave toward the oncoming plasma. The gun is at port 1 (Figure 8) in the median plane.

Two actions cause penetration of the field by the plasma: First, the cloud's ions are deflected in the magnetic field in one direction while the electron component of the plasma bends in the opposite direction. This charge separation produces opposite charges on the opposite boundaries of the finite sized cloud of particles. Only enough charge particle density is necessary to make the dielectric constant $K=1+4\pi n M_i c^2/B^2 = 2$ for the resulting polarization electric field to be sufficient to cancel the magnetic force on the moving collimated ions, where M_i is the ion mass and n is the number of ions per cubic centimeter. The interior of the cloud can thus drift across the magnetic field with its field-free flight speed:[9] $v=cE/B$. This action has provided a θ dependent electric field which temporarily destroys absolute containment or absolute exclusion. Second, the configuration is unstable inwardly to flute generation where the lines of force are concave toward the oncoming plasma. Thus the grad B drifts in the entering plasma cloud, which is equivalent to the protruding flute, add charge separation and cause more polarization electric field thereby aiding the plasma entrance by this inward instability. The plasma does not enter by displacing the magnetic field by diamagnetic pressure -- there is practically no tranverse

pressure in a collimated beam.

We can estimate the ratio of these two polarizing currents. To form the polarizing field $E = (v/c)B$, we need $I_P = \sigma Av/(cL)$ e.m.u. of current if A is the area of the charged side of the cloud, L is the length of the cloud, v the drift velocity of the cloud, and σ the charge per unit area. The current due to a grad B drift is:

$$I_G \sim (A n w_I a\, e/c \quad (\nabla |B| /B)$$

where w_I is the velocity of a particle in the cloud perpendicular to the $\vec{E} \times \vec{B}$ drift and a is its gyroradius. The ratio, $I_P / I_G \sim (v/w_I)(v/c)(B/\{a \nabla |B|\})(B/\{nL\})(2 \times 10^8)$. With $v/w_I \sim 10$, $v/c = 3 \times 10^{-4}$, $B/\{a \nabla |B|\} \sim 10$, we find

$$I_P/I_G \sim 10^7 \; B/(nL). \qquad (2)$$

In our entrance field of approximately 10^3 gauss, $I_P \sim I_G$ provided $nL = 10^{10}$. Thus the gradient B charge separation current can contribute much of the polarization for an injected stream of plasma with densities of 10^{12} with penetrations or flutes of only a fraction of a centimeter during injection.

An estimate can also be made of the possibility that a small group of particles with a nonisotropic velocity distribution causes a large loss of already trapped plasma which

has an isotropic velocity distribution. The small directed group, of density n_1 - if it should succeed in generating a polarization electric field - would start to drift out of the confined plasma by forming a flute and taking along all the other particles of density n. However the $\nabla|B|$ drift of all the particles in the flute protruding into an increasing field, B_1, discharges the electric field and stops flute growth. The loss in directed energy in moving all the particles with orbital magnetic moment, μ, to B_1 from B_o is $n\mu(B_1-B_o)$. The directed kinetic energy, $(1/2\ n_1 M v_1^2$, is removed when $(B_1-B_o)/B_o = 1/2\ (n_1/n)(v_1/\omega_I)^2$. Thus for trapped plasma with $v_1/\omega_I=1$, an n_1 10% of n would not cause a loss of plasma but would merely flute to reach a field 5% greater.

Since a nonisotropic velocity distribution enables plasma to enter the confining region, we can equally well expect some groups of plasma particles to polarize and to escape across the field at early times before the grad B drift of background particles has built up. Observations showing just such occurrences will be described in Section V on transit.

After the plasma enters by polarization, the stream of plasma is prevented from continuing on across the multipole and out through the field on the other side by the propagation of potential along field lines. The lines of force encircling an

outer hoop are crossed by the plasma stream first where these lines are directed downwardly; and farther in, the stream meets the same lines directed upwardly. At the first encounter, a polarization occurs in the plasma of a polarity which provides the inward E x B drift. To continue across the line of force a second time requires an opposite polarity because the direction of the line of force is now upward. Swift discharge of the original polarization field by flow of electrons along the line of force would result from the attempt of continued motion of the plasma stream inward. Thus the innermost plasma is brought to rest by the flow of this depolarization current. The plasma stream has short circuited itself by moving into a reversed field composed of the same lines of force it crossed on entry[5] (Figure 9).

The same comments hold for the lines of force outside $\psi=0$ which pass around all four hoops. The plasma would encounter these lines a second time if it crossed the center of the octupole, but the discharge path in this case is long.

The observations bearing on the expectations just described were carried out by probes of two types, Figure 10. Densities of plasma were determined by the saturated ion current between the electrodes of the low impedance floating double probe. Floating potential, V_f, was determined by one of the electrodes on a high impedance floating double probe. The impedance

between the electrode tip and ground was 10^6 ohms and the frequency response was good up to 5 megacycles. Electric fields were read by the difference signal between the two electrodes of this probe. The impedance of this circuit was 2×10^6 ohms with a 5 megacycle frequency response. The common mode rejection was always over 100 to 1.

These probes entered the plasma at the numerous ports through ball swivel joints bearing on Viton "O" rings. Scales outside the vacuum chamber gave the three coordinates which were converted by tables to the coordinates, $\int$, ϕ, and θ, of the tip of the probe within the plasma. In addition, the probe could be twisted to give E_θ or some other components of the electric field.(Figure 8)

Polaroid pictures of the oscillograph traces were reduced to the graphs of data presented here either by eye piece measurement, or, for cases of voluminous data, by digitizing the traces and using a digital computer to interpolate, to collate, and to draw the graphs. Digitizing was done by means of the high energy particle physics group's track measuring equipment applied to oscillograph traces.

The first effect, namely polarization of the plasma as it entered the magnetic field, is shown in Figure 11. The floating potential is shown. It has the correct polarity and the magni-

tude of the inward drift velocity calculated from $v_o = cE/B$ is $\sim 1.2 \times 10^7$ cm/sec. This agrees with the 1.2×10^7 cm/sec speed of the plasma in the field-free region between the gun and the multipole.

Next the density distribution in the direction of the stream within the multipole is shown in Figure 12. At early times the density was high ($\sim 10^{12}$) just within the entrance. Later it built up farther in near the zero field position, but practically no plasma got more than 5 cm beyond the zero field point. It was stopped before it reached the center by the self short circuiting effect on the lines around the outer hoops and by spreading around in the θ direction. Furthermore, plasma entering late and encountering the short circuited initial segment of the stream should split and pass to the $+\theta$ and to the $-\theta$ sides of the initial segment because the direction of the electric field causing drift would be turned from the θ direction to the r direction by the short circuited stopped plasma.

To cause the capture of the plasma, a short circuit depolarizing current, $J_{\parallel}$, should flow along the lines of force under the hoops, and a resulting $J_{\perp}$ B force would remove the directed momentum of the plasma. Figure 13 shows the current determined by a Rogowski loop or current transformer circling these lines of force. Calculation of the impulse absorbed by the J x B

force using the J_1, which was also measured by the Rogowski loop and which flows to attempt to recharge the depolarized plasma showed it was great enough to stop the stream of density 10^{12} cm. $^{-3}$ in the 2 microseconds observed.

On the opposite side of the low field region from the injection port, electric fields occurred in spite of the lack of much plasma density. The potentials, V_f of Figure 11, just inside from the injection port might be expected to propagate along the lines of force outside $\psi = 0$ to the opposite side of the multipole. Figure 14 shows that the resulting E_θ changed sign suddenly. First the plasma penetrated toward the wall according to the sign of E_θ; then in suddenly reversed direction and moved inward. In this same region opposite the injection port, a few energetic ions overshot their associated electrons and caused a large radial potential gradient, Figure 15. This has also been observed in linear octupole test sections.[16]

V. Transit of Plasma Around The Octupole

The collection of plasma, which built up inside the

injection port behind the short circuited front of the plasma stream lost its inward momentum and spread in both directions around the toroid. The detectors for this motion were also the floating double probes used to determine density, electric field, and floating potential. There were eight probe positions normally available (Figure 8). Vacuum locks allowed the rapid interchange of probes. At some interesting times and regions, the plasma to probe electrode impedance was found to approach 2×10^5 ohms. Both the 2×10^6 ohm high impedance and the 5 MHz high frequency response were important for observations needed to determine the motion.

The construction of hoop supports was such that the hoops could be insulated from the multipole wall, connected to the wall, or biased at a potential. The possibility that potentials applied to the hoops might influence the motion of a plasma cloud during filling was investigated.

With a linear multipole structure, the two-dimensional magnetic field plot would be orthogonal to and coincident with an electric field flux plot formed by holding all the current-carrying rods at an electrostatic potential relative to the wall. Single particles in this structure would then travel lengthwise with the $\vec{E} \times \vec{B}$ drift of the same magnitude and direction at all points. In the three-dimensional toroidal case, magnetic field lines are not equivalent to electrostatic potential lines as they are for problems in two dimensions with a voltage on the hoops. Nevertheless, the $\vec{E} \times \vec{B}$ drift in a toroidal multipole would be circumferential.

Little influence on the plasma motion during filling has been observed due to applied hoop potentials. First of all, the plasma splits at the injection port and goes both ways around the octupole. If it were guided by hoop potential, it could drift only one way . Secondly, potentials, applied or acquired by the hoops, would tend to be shielded by the plasma itself. The electrostatic boundary conditions would then be noticeable only close to the conductors where the plasma is very tenuous. In this close region,

$\vec{E} \times \vec{B}$ drifts would be parallel to the wall.

Figure 16 shows what actually happened. The floating potential in the plasma formed reversed octupole patterns providing $\vec{E} \times \vec{B}$ drifts around the toroid in each direction. Numerical comparison of cE/B and the observed flow velocity of the plasma around the toroid is shown in Figure 17. Apparently the plasma moved circumferentially as though unimpeded by the magnetic field with a speed near to that in the field-free drift space between the gun and exterior multipole wall.[6] With the multipole field off, plasma did not appear at port 5, 180° around the toroid from the injection port.

Potential readings at ρ=12.5 cm and ϕ=80°, below the point of zero field for various azimuths or θ's showed opposite polarity potential waves traveling in opposite directions from the injection port 1 to the collision point near ports 4 and 5 (Figure 18). This plot does not have many points on it, but for each

observation at each port, there is also knowledge of $\partial V_f/\partial t$ which allows estimation of $\partial V_f/\partial \theta$ from $(v/R)\,\partial V_f/\partial \theta = \partial V_f/\partial t$. Thus slopes are known.

When the waves of opposite potential approached at the collision point, an E_θ was created. This E_θ was in such a direction to throw the plasma toward the outer wall in each lobe of the octupole. Figure 19 shows the motion of the mass of plasma with time, and it also shows that the plasma mass moved close to the top and bottom walls at the collision azimuth.

The electric field in the circumferential direction which appeared at the collision point causing outward drift of plasma must be accompanied by a reverse electric field as azimuths other than the collision point since $\oint \vec{E} \cdot \vec{dl} = 0$ where dl was along a circle about the major axis. This is true to the extent that the magnetic flux linkage was not changing in time during the experiment. Thus while plasma moved outward at the collision region it must move inward by E x B

drifts at some other azimuths.

Figure 20 shows potentials and densities as the cloud was passing a port at $\theta = 50°$ to the right of the injection port. The velocity of the cloud past the 50° port as calculated from the observed electric field is shown in Figure 21. The speed was very close to that of the plasma in field-free space except that particles at the edge which engage in establishing the observed electric field perpendicular to ψ lines had no velocity and particles outside the forward moving cloud actually would drift backwards.

An idea of the flow in the form of a motion picture is given in Figure 22. Equipotential lines are shown around portions of plasma, and the flow of plasma follows these equipotential lines since it is dominated by E x B drifts. To obtain data for flow in the whole confinement region it was necessary to make simultaneous observations at many ports. There were ten oscilloscope traces made on each pulse in many of these tests. Polariod photographs provided data for immediate judgement of results. The traces on the polaroid pictures were measured and digitized as explained previously.

Several examples of the generation of radio frequency E_θ signals were discovered with frequencies in the range of one to several megacycles per second. (Figure 23). In all cases, these wave trains commenced when ∇n, the density gradient, was reversed from the gradient necessary for stability with the maximum pressure at the separatrix of the flux plot. Although this

was during the filling time before a steady state was established, the phenomenon was probably associated with the redistribution of plasma density by the process of inward flute growth.

Another observation which was made during plasma flow showed energetic ions striking the vacuum box wall perpendicularly. The electrostatic ion energy analyzer receiving ions emerging normally through a hole in the wall showed some plasma escape at the time and place of collision (Figure 24), and at other azimuths usually in bursts during the first 50 microseconds, but in some cases up to $\sim$150 microseconds. The only way ions could hit the wall perpendicularly was for them to be influenced by a tangential electric field, E_θ, of sufficient magnitude to separate the drifting particles' orbit loops. The electric field close to the wall must be perpendicular to the wall, thereby allowing drift only parallel to the wall. Thus it was essential that an E_θ be present approximately a gyroradius away from the wall

to cause these escaping orbits. This E_θ was observed with the proper magnitude to separate orbit loops at the time of particle escape.[17] After 100 microseconds measured from the time of gun current, the plasma was not flowing and the detector did not observe ion escape to the wall. The energy distribution of particles which struck the wall was similar to the distribution from the plasma gun (Figure 7).

The question of how the plasma was guided around a circular path in the toroid arises because the plasma cloud was injected by forming a local E_θ. Why would it not be possible for the plasma cloud to retain its organization within the confining region so it could again cause an E_θ and escape instead of following a circular path in the toroid? This may happen to some parts of the plasma at some times, but the tendency for magnetic lines of force to be at single electrostatic potentials forces the plasma to move on the average in a circumferential direction. The cloud could expand on all sides toward the wall or recede on all sides from the wall; but during

filling, tangential motion as a whole toward the outside generates depolarizing currents which provide the J_c x B force to give the centripetal acceleration needed to cause circumferential motion. Attempts to measure this guiding current density were difficult because of the larger current density in the same regions needed to confine the plasma pressure. Roughly the ratio would be expected to be $J_c/J_p \sim \rho/R$ where J_c and J_p are respectively the current density for supplying centripetal force and J_p that for confining the plasma pressure. ρ is the minor plasma toroid radius and R is the major toroid radius.

VI. Confinement Time

Several methods of observing the plasma lifetime have been used in the course of these experiments. The first method used Langmuir probes.[6] They showed that plasma was present from the time of injection to the time the magnetic field disappeared - about 3.0 milliseconds later. The mean life of the plasma was 0.6 to 0.7 milliseconds as shown in Figure 25. The saturated ion current shown was taken as a measure of the ion density which decayed from an initial value of 10^9 cm^{-3} after the filling transient past. At the time of these observations the fact that the ions retained their speeds or temperature was not known with certainty so other measurements were needed to be certain that saturated ion current was proportional to density. However, the Langmuir probes demonstrated that the electron temperature remained $\sim$10 eV from the time of injection on (Figure 26). The decrease of plasma density with time was smooth and gave no evidence that a sudden loss of plasma occured such as the

onset of an instability might produce. Furthermore the calculated mean life for loss of 100 eV protons on the small hoop supports was 0.5 milliseconds. The slightly longer lifetime observed by Langmuir probes could well be due to the presence of ions down to 50 eV in the distribution of ion energies. (Figure 7)

A second observation of containment was made by 3 cm wave length electromagnetic radiation. For low densities the fractional shift in the resonant frequencies of the vacuum toroid is $\Delta f/f = 1/2\ \bar{n}/n_o$. where $\bar{n}$ is the average plasma density in the cavity, n_o is the density for which f is the plasma frequency and Δf is the shift in the resonant frequencies. The measurement was made by setting the frequency of a klystron on the slope of a resonance. The addition of plasma raised (or lowered) the amplitude of the response by shifting the resonant frequency of the cavity, while the response is not linear for large frequency changes, the method can be used as an indicator of electron density. Figure 27 shows the electron component of the plasma remaining throughout the duration of the

magnetic field. The magnitude of the frequency shift indicated a density of $n \sim 10^9$ cm^{-3} in the plasma region in agreement with Langmuir probe determinations.[7]

The third measurement was a direct determination of ion lifetime as a function of ion energy.[19] This was accomplished by extracting ions directly from deep within the plasma and bringing them out to the electrostatic ion energy analyzer. After filling, the floating potential remained near zero. Hence it would not alter the ion spectrum during lifetime observations. A long 6 mm iron tube with 0.5 mm walls provided a field-free channel shielded from the 800 gauss to 2000 gauss fields through which the ions were extracted. The mean life of 100 eV ions was about 0.4 milliseconds with the iron tube and the hoop supports immersed in the plasma. This agrees well with the 0.5 millisecond life calculated for 100 eV ions striking the hoop support area.

The number of ions extracted had the exponential shape shown in Figure 28 with no sudden plasma losses, and the mean life of a particular ion energy was inversely proportional to the ion velocity, as it should be if the loss is on the hoop supports. (Figure 29) This behavior was

what would be expected of a stable plasma.

As the background pressure was raised to 10^{-5} torr the ion lifetime was finally affected (Figure 30). However this pressure was more than a factor of 10 greater than normal background gas pressure (4×10^{-7} torr) before a noticeable change was made in ion lifetime. The firing of the plasma gun introduced gas which was observed to raise the pressure in the multipole chamber to 10^{-5} torr in 2 milliseconds if the gas shutter was not closed. Thus gas pressure increase is not expected to be an influence on plasma lifetime in these experiments, as it apparently was in some cases with more plasma density. [20]

VII. Discussion

The data are not as detailed as desired to give a very accurate determination of the efficiency of capture or retention of the plasma after it has entered the injection port; but what is known indicates that the capture is greater than 10%. When the detail and accuracy of velocity and density measurements is sufficient to satisfy a continuity equation for plasma motion, the efficiency of capture and the regions of loss during filling will be known. How much of the plasma is turned back at the collision point and how much hits the wall, are not now known.

An interesting characteristic of the plasma of energetic ions which becomes quiescent after 50 to 100 microseconds and which remains for a couple of milliseconds while the magnetic field is decreasing is that any electrostatic potential variations at the boundary of the plasma are much smaller than the ion energies present. The large potentials are apparently present only in the period of plasma motion across the magnetic

field and for ~50 microseconds thereafter. It is necessary to know more than is now known about the distribution functions of electrons and ions to properly interpret the floating potentials which are measured. The difference between plasma potentials and floating potential is usually taken as ~3 times the electron temperature, but this electron temperature may be different in the center and at the edge of the plasma. The processes enabling the plasma to evolve into this state of small electric fields at its edges remain to be examined by further experiments.

Another detail needing examination is the process of entry through the slotted wall. When the plasma passes through the slots, the lines of force have already diffused into the aluminum and hence the slots are crossed by field lines in contact with and short circuited by the aluminum bars forming the slots. This condition would be expected to lead to a depolarization of the plasma. Measurements show very little alteration of the magnetic field near the slots when plasma is injected. The ion gyroradii are larger than the thickness of short circuited magnetic field region and because of this ions may be able to pass through and to cause the positive potential at the left just inside the in-

jection port while very little potential of the opposite sign is generated just inside at the right of the port. (Figure 11)

The energetic ion lifetime was independent of the amplitude of magnetic field near the usual operating field. This should be true if the gyroradius of ions is about the size of the hoop hangers or larger. However if the ion gyroradius is small compared to the width of the hangers, the lifetime should be proportional to B. It may be possible to reach sufficiently high field strengths in the future.

This experiment may have escaped troubles with charge exchange loss due to gas released when the plasma is injected into the octupole. There are two reasons: first, our injected stream density was probably less than that for cases where charge exchange seems to have limited lifetime;[20] second, our wall slots line up with the open slots in the gas shutter. Thus liberation of gas by fast collimated plasma striking metal occurs mainly at the shutter which is 12 cm from the entrance to the octupole space. Gas produced at this shutter has a good opportunity to flow back into the large differential pumping chamber.

Acknowledgments

We would like to acknowledge the help of G. O. Barney, Walter Grengg, J. C. Sprott, D. E. Lencioni, Reinhardt L. Willig, and Glenn Kuswa in construction and operation; and Professor K. R. Symon, P. C. T. van der Laan, and Professor George Schmidt for extensive discussions. Professor U. Camerini's help in adapting strange particle track measuring equipment to our data handling problem and the assistance of Professor J. B. Beyer of the Electrical Engineering Department, with microwave problems were especially appreciated.

Footnotes

1. J. Berkowitz, K. O. Friedrichs, H. Goertzel, H. Grad, J. Killeen, and E. Rubin, Proc. Second U. N. Conf. Peaceful Uses of Atomic Energy, Geneva, Vol. 31, p. 171, (1958)

J. Berkowitz, H. Grad, and H. Hubin, Proc. Second U.N. Conf., Peaceful Uses of Atomic Energy, Vol. 31, p. 177, (1958)

J. L. Tuck, Proc. Second U. N. Conf., Peaceful Uses of Atomic Energy, Vol. 32, p. 3 (1958)

US AEC Report, Washington, Vol. 184, p. 77, (1955)

H. Grad, US AEC Report, Washington, No. 289, (1955), p. 155, and N. Y. O. 7964 (1957)

2. B. B. Kadomtsev, "Plasma Physics and the Problem of Controlled Thermonuclear Reactions", (Pergamon Press, N.Y.) Vol. IV, p. 425.

S. I. Braginskii, and B. B. Kadomtsev, "Plasma Physics and the Problem of Controlled Thermonuclear Reactions", (Pergamon Press, N. Y.) Vol. III, p. 356.

B. B. Kadomtsev, S. I. Braginskii, Proc. Second. Intl. Conf., Peaceful Uses of Atomic Energy, Vol. 32, p. 233 (1958)

3. J. L. Tuck, Nature, Vol. 187, p. 863, (1960)

4. T. Ohkawa, D. W. Kerst, Phys. Review Letters, Vol. 7, p. 41, (1961)

Il Nuovo Cimento XXII (4), p. 784, (1961)

5. D. W. Kerst, Bull. Am. Phys. Society. II, Vol. 7. p. 139, (1962)

G. O. Barney, W. E. Wilson, R. A. Dory, D. W. Kerst, Bull. Am. Phys. Society, II, Vol. 8, p. 521, (1963)

6. W. E. Wilson, D. M. Meade, Bull. Am. Phys. Society, II, Vol. 9, p. 495, (1964)

7. W. E. Wilson and D. M. Meade, Bull. Am. Phys. Society, II, Vol. 9, p. 532, (1964) Abstract B9

D. M. Meade and W. E. Wilson, Bull. Am. Phys. Society, II, Vol. 9, p. 532, (1964) Abstract B10

8. Private Communication.

9. D. A. Baker, J. E. Hammel, Phys. Fluids, Vol. 8, p. 713, (1965)

10. H. P. Eubank, T. D. Wilkerson, Rev. Sci. Inst., Vol. 34, p. 12, (1963)

11. T. T. Cook, R. A. Dory, "Field Design for a Toroidal Multipole Plasma Device", Bull. Am. Phys. Society, Vol. 7, p. 521, (1963)

12. H. P. Furth, M. N. Rosenbluth, Phys. Fluids, Vol. 7, p. 764, (1964)

J. L. Johnson, Phys. Fluids, Vol. 7, p. 2015 (1964)

13. These arguments on absolute containment are due to G. R. North.

14. W. Josephson, Journ. Applied Phys., Vol. 29, p. 30, (1958)

F. R. Scott, H. G. Voorhies, Phys. Fluids, Vol. 4, p. 600 (1961)

15. G. Kuswa, submitted to R.S.I. for publication.

16. T. Ohkawa, A. A. Schupp Jr., H. G. Voorhies, W. C. Duesterhoeft Jr., Phys. Fluids, Vol. 6, p. 1526 (1963)

17. C. W. Erickson, D. M. Meade, Bull, Am. Phys. Soc. II, Vol. 10, p. 235, (1965)

18. T. Ohkawa, M. Yoshikawa, A. A. Schupp Jr., H. G. Voorhies.

Bull. Am. Phys. Society II, Vol. 10, p. 197 (1965)

19. D. W. Kerst, R. A. Dory, W. E. Wilson, D. M. Meade, C. W. Erickson, Phys. Review Ltrs., Vol. 15, p. 396 (1965)

20. T. Ohkawa, A. A. Schupp Jr., M. Yoshikawa, H. G. Voorhies, Sec. Int'l. Atomic Conf. on Plasma Physics and Controlled Nuclear Fusion Research, Culham.

CAPTIONS

Figure 1a. Quadrupole "Cusp" with lines of force returning around current-carrying rods. The cusp configuration is seen at the center. The last flux line with magnetohydrodynamic stability is labeled ψ_c.

Figure 1b. Octupole field with all rod currents in the same direction and return current in the wall. A stable plasma has its maximum pressure on the $\psi = 0$ line as shading indicates. The last stable line is ψ_c. Plasma pressure must decrease from $\psi=0$ to ψ_c for stability.

Figure 2. Apparatus. The plasma gun is at the right. The maximum excitation would provide 9.6 gyroradii across the plasma at outer hoops and 20 gyroradii at inner hoops for 100 eV protons. Most observations were made at half this exitation.

Figure 3a. Flux plot for rectangular toroidal conducting wall with hoop sizes and positions chosen to give one minimum B at $\psi = 0$. 70% of the ten flux tubes are in the stable region.

Figure 3b. Plot with corners cut from wall. 80% of the flux is in the stable region. $\psi_{wall} - \psi_{rod} = 10$.

Figure 3c. Plot with corners cut off and walls filled in. 90% of the flux is stable.

Figure 3d. Linear Octupole plot for comparison with 3b. Note the lack of distortion in 3b in spite of the fat aspect of the toroid.

Figure 4. The volume of a unit tube of flux, $dV(\psi)/d\psi$, as a function of ψ. The last magnetohydrodynamically stable flux line is ψ_c where the volume of unit tube of flux is minimum. ψ_w is at the wall and $\psi=0$ is the separatrix of the flux plot.

Figure 5. Magnetic field in gauss along the central vertical line through the vacuum box and along the median plane. The maximum field amplitude in the box for this excitation is at the surface of inner hoops and it is 11,000 gauss.

Figure 6. Absolute containment zones for the same particle momentum, P, but for different values of P_θ. The zero field minimum is thus enclosed in an absolute

containment zone, 6b, and it is surrounded by other absolute containment zones, 6a and 6c, having high B and thus constant orbit magnetic moments μ.

Figure 7. Proton Energy Spectrum from the plasma gun.

Figure 8. Arrangement of probe and injection ports as seen from above and definitions of the coordinates ρ, $\emptyset$, θ of points at which observations are made. Swivel probes allow exploration in the circumferential, or θ direction between ports. The magnetic field direction is down at the outer wall.

Figure 9. The same lines of force around the rods are crossed twice as the injected plasma stream enters. At the second crossing, the attempt to generate reverse polarization potential on the same line of force results in discharge $J_{//}$, of the initial polarization and a current, $J_{\perp}$, which stops the forward motion of the plasma by $J_{\perp}B$ force.

Figure 10. Probes -- a) High impedance with frequency response to 5 mc is obtained by installing the resistance of a resistance - capacitance divider at the electrode

of the probe. Capacitance c and c' are stray. The dividers are separately balanced.

b) Low impedance probe for determining the plasma density.

Figure 11. Floating potential a little distance inside the injection port. Positive θ is to the right. The gradient of this potential gives the polarization electric field generated by the plasma crossing the magnetic field as it enters.

Figure 12. Plasma density distribution after passing through the injection port. Plasma penetrates from the right but only a small amount travels a few centimeters beyond the zero field point at $\int=0$. All times are measured from the time of the start of plasma gun current.

Figure 13. Depolarization current parallel to the lines of force looping the outer hoops. See Figure 9.

Figure 14. Theta component of the electric field at different points across the toroid at the injection azimuth. Injection occurs at the right at 10.4 microseconds. The electric field at the port gives an inward entrance velocity $\sim 10^7$ cm./sec., $\sim$ field free plasma cloud speed.

At 13 microseconds, the electric field near the wall opposite the injection port shows a large outward velocity which at 14.4 microseconds suddenly reverses and turns the plasma inward toward the zero field locus, $\int = 0$.

Figure 15. The high potential near the wall opposite the injection port is caused by a small number of ions overshooting their associated electrons. Practically no plasma passes the -5 cm. point. (See Figure 12)

Figure 16. Octupole Floating potentials. Upper - The potentials on a 10 cm. radius circle about the zero field point +50° to the right of the injection port. Lower - Potentials on the cloud at -50° moving to the left of the injection port. Hoops are at $\Phi = 45°$ and $\Phi = 135°$

Figure 17. Velocity of drift around the toroid calculated from E_{θ}/B_{φ} of Figure 16 for the time 14 microseconds after the gun fires. The speed of travel around the toroid observed by plasma density probes is

1.2×10^7 cm./sec., the same as that in a field-free region. The calculated drift velocity in this instance is somewhat less.

Figure 18. Floating potential as a function of θ or azimuth around toroid. Two potential waves of opposite polarity were generated by the injected plasma splitting and progressing in opposite θ directions. The potentials were on a circle of different θ values at $\int$ = 12.5 cm., ϕ = 80° which was below the B = 0 circle. Injection is at θ = 0°~360°, and the potential waves progressed to collision about 21. microseconds after gun firing. Note the large potential gradient in the θ direction at the collision. This E_θ carried plasma out toward the wall.

Figure 19. Density of plasma at the collision of the two streams of plasma 180° around the toroid from the injection port. The plasma arrived in the low field region and then spread toward the walls -- in this case the top and bottom walls -- at 30 microseconds. Electric fields close to the conducting wall must be normal to the wall causing drift along the wall and away from the collision as in Figure 21.

Figure 20. Floating potential and density in the median plane at $\theta = 50°$ for different times. The reverse potential gradient at the outer edges would cause any plasma there to drift backward.

Figure 21. The calculated drift velocity, $v=cE/B$, as a function of position across the median plane at 50° and at 15 microseconds (see Figure 20). Note the reverse drift velocity at the edges.

Figure 22. Sequence of views of the plasma clouds from formation by splitting at injection to collision at 180°.

(a) 11 microseconds, injected stream stops near B=0 line by depolarizing on lines of force looping over rods. Equipotential lines are given drift arrows since E x B flow is parallel to these lines. Plasma splits on the short circuit near B = 0.

(b) 15 microseconds, plasma begins to flow in opposite directions generating the octupole electric field.

(c) 20 microseconds, plasma spreads around toroidal chamber.

(d) 25 microseconds, oppositely directed plas-

ma clouds approach at 180° and potentials cause E_θ field driving "colliding" plasma outward toward wall.

(e) 35 microseconds, plasma has moved out and backward along wall by $\vec{E} \times \vec{B}$ drifts.

Figure 23. Photograph of oscillographic trace of radio-frequency E_θ at a point where the density gradient is instantaneously reversed from the proper direction for stability.

Figure 24. Ions of 160 eV energy emerging perpendicularly through a hole in the wall. A brief burst occurs at the collision time, 21 microseconds, and occasional particles come out over the subsequent 100-200 microseconds. Sweep-speed is 20 microseconds per division.

Figure 25. Floating double probe saturated ion current which measures plasma density as a function of time. No sudden plasma loss was evident in the oscillograph data.

Figure 26. Langmuir probe traces at early and at late times giving $\sim$10 eV electron temperature for the whole period. For the probe electrodes used, the extropulation of the square of electron current as a function of voltage gave the temperature.[6]

Figure 27. Indication of average electron density by amplitude of response of cavity to 3 cm. electromagnetic waves. The Klystron is tuned to be on the slope at the side of a resonance so addition of electrons to the cavity space changes the response. Sweepspeed is .5 milliseconds per division. Plasma is injected after the field has risen for one millisecond. The detector output is shown for cases of no plasma injected and plasma injected.

Figure 28. Total ions of 102 eV collected by ion extractor as a function of time. The curve is exponential. Sweepspeed is 200 microseconds per division. Roughness is due to counting statistics.

Figure 29. Ion mean lifetime as a function of ion energy. The solid line is the curve for lifetime proportional to reciprocal ion velocity such as for the case of ions hitting the hoop hangers or probes.

Figure 30. Lifetime of 126 volt hydrogen ions as a function of background pressure. Normal operating pressure was $\sim 4 \times 10^{-7}$ torr and firing the plasma gun brings the pressure to 10^{-5} torr in 2 milliseconds without the gas shutter being operated.

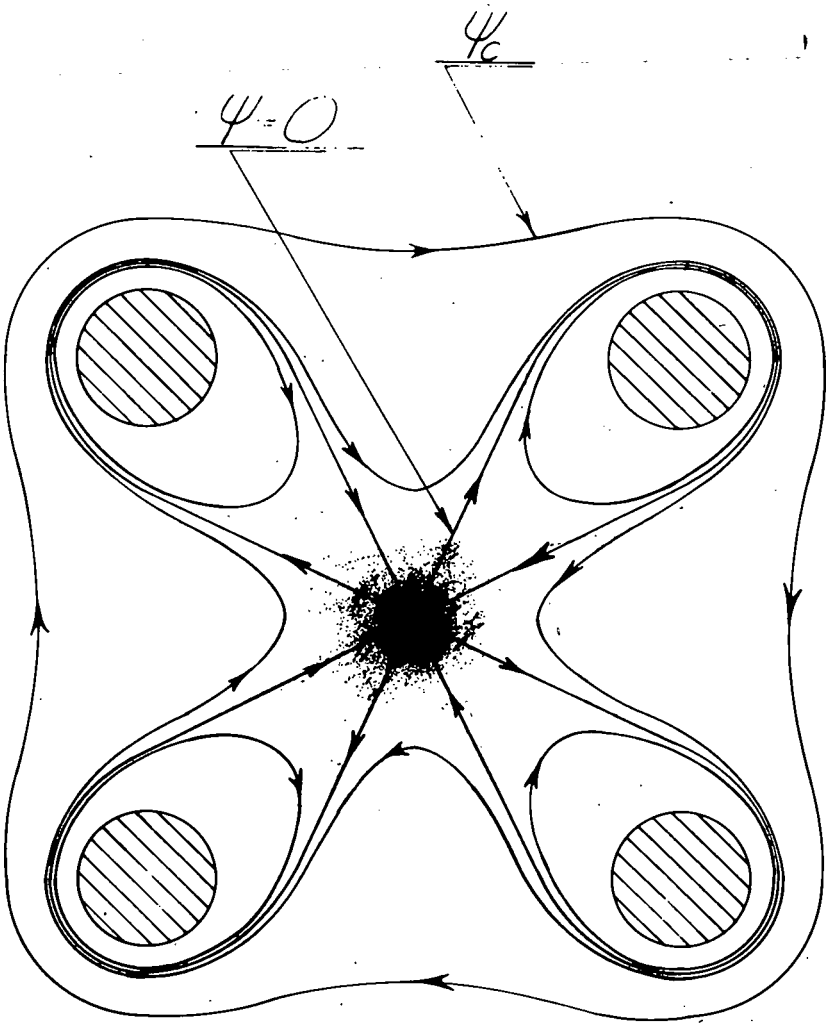

FIG. Nº 1b

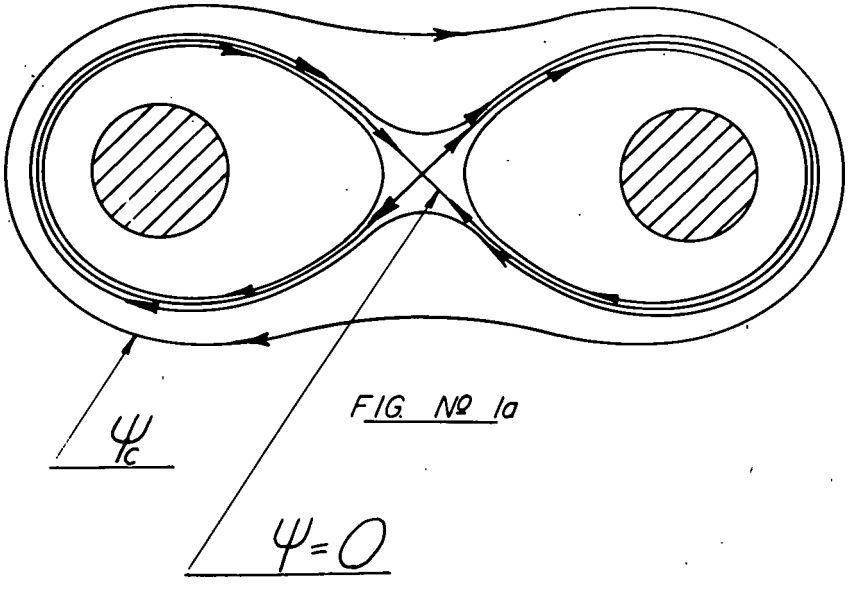

FIG. Nº 1a

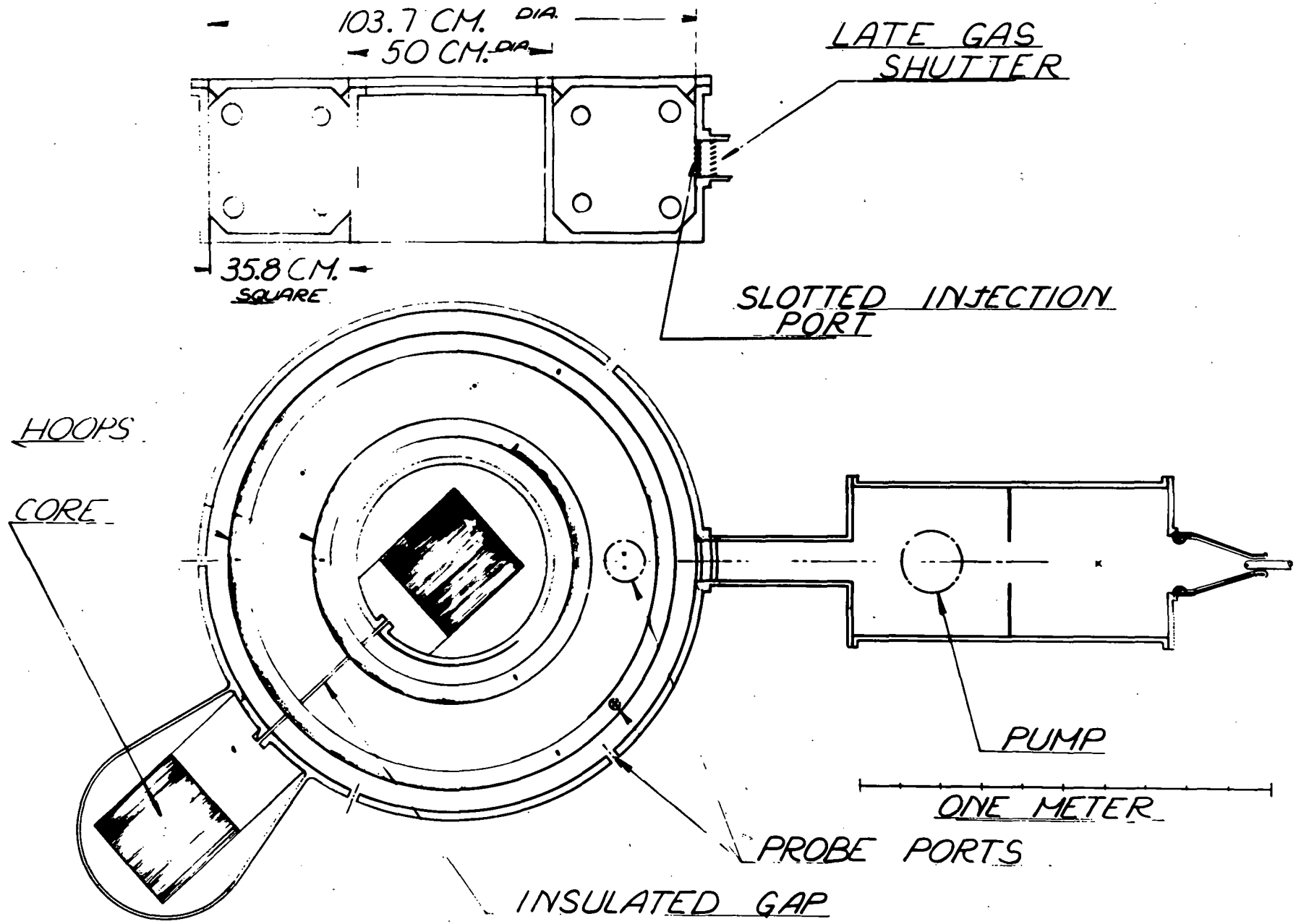
103.7 CM. DIA.
50 CM. DIA.
LATE GAS SHUTTER
35.8 CM. SQUARE
SLOTTED INJECTION PORT
HOOPS
CORE
PUMP
ONE METER
PROBE PORTS
INSULATED GAP

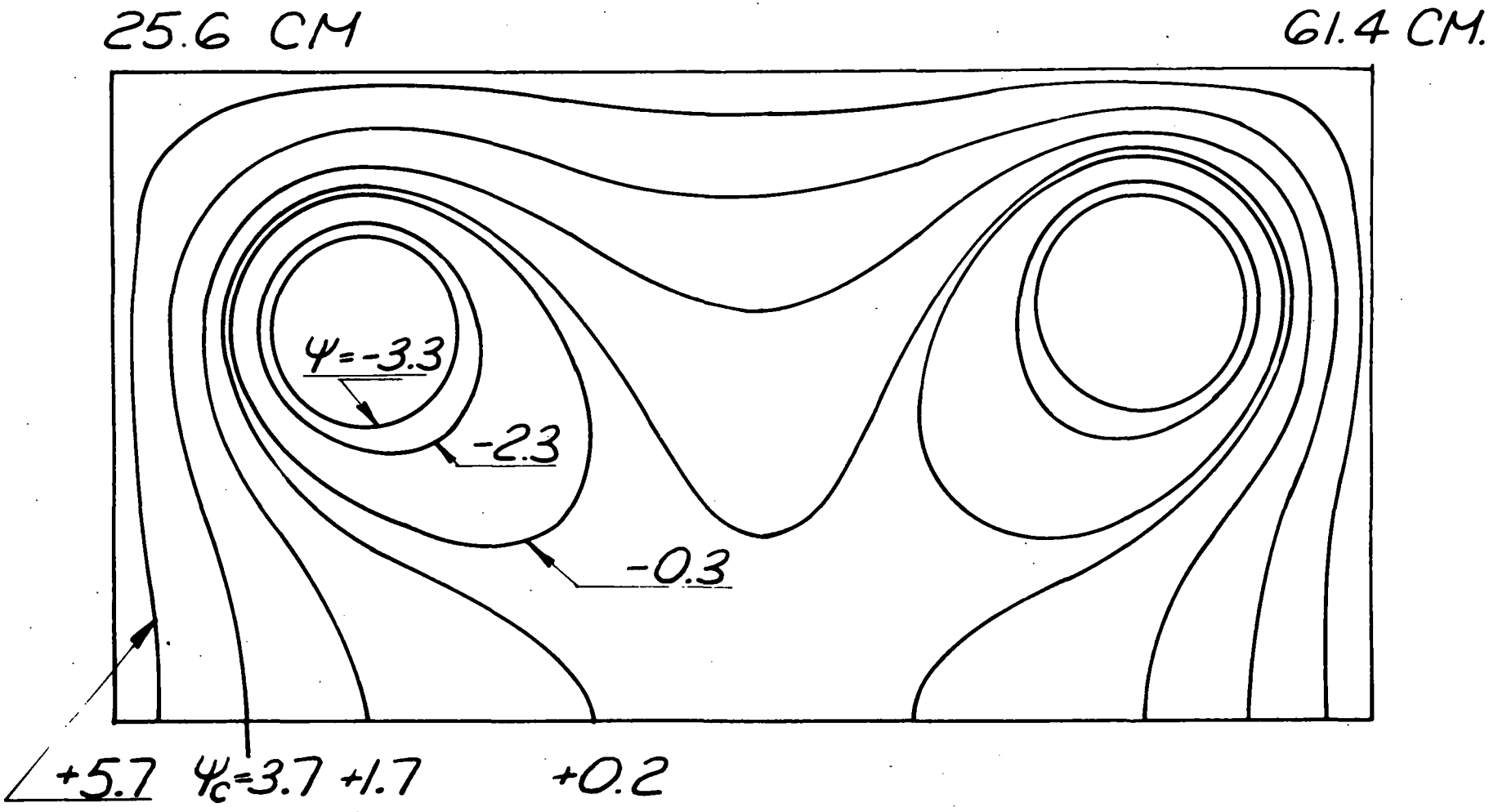

FIG 3A

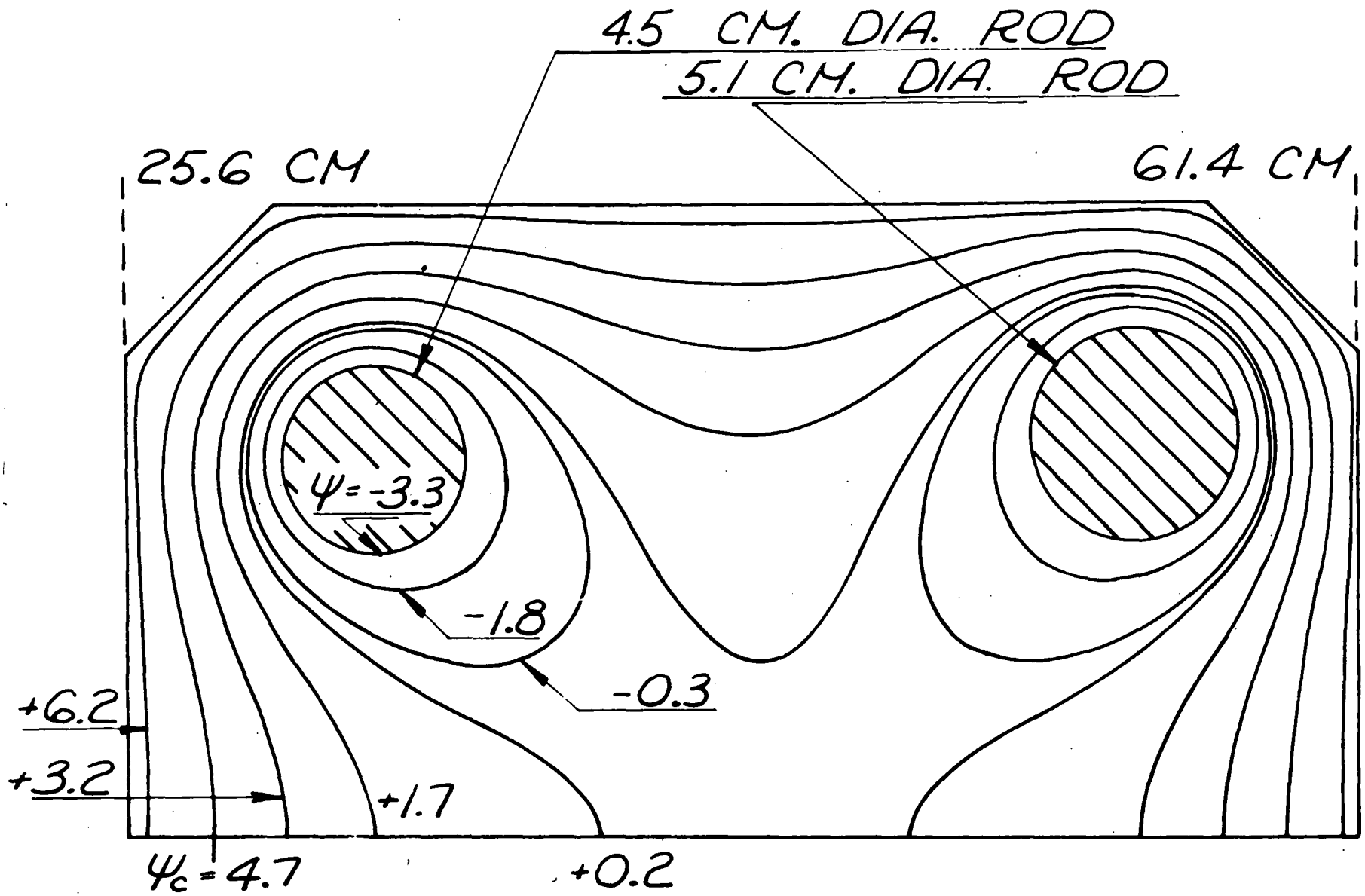

Fig. 3B

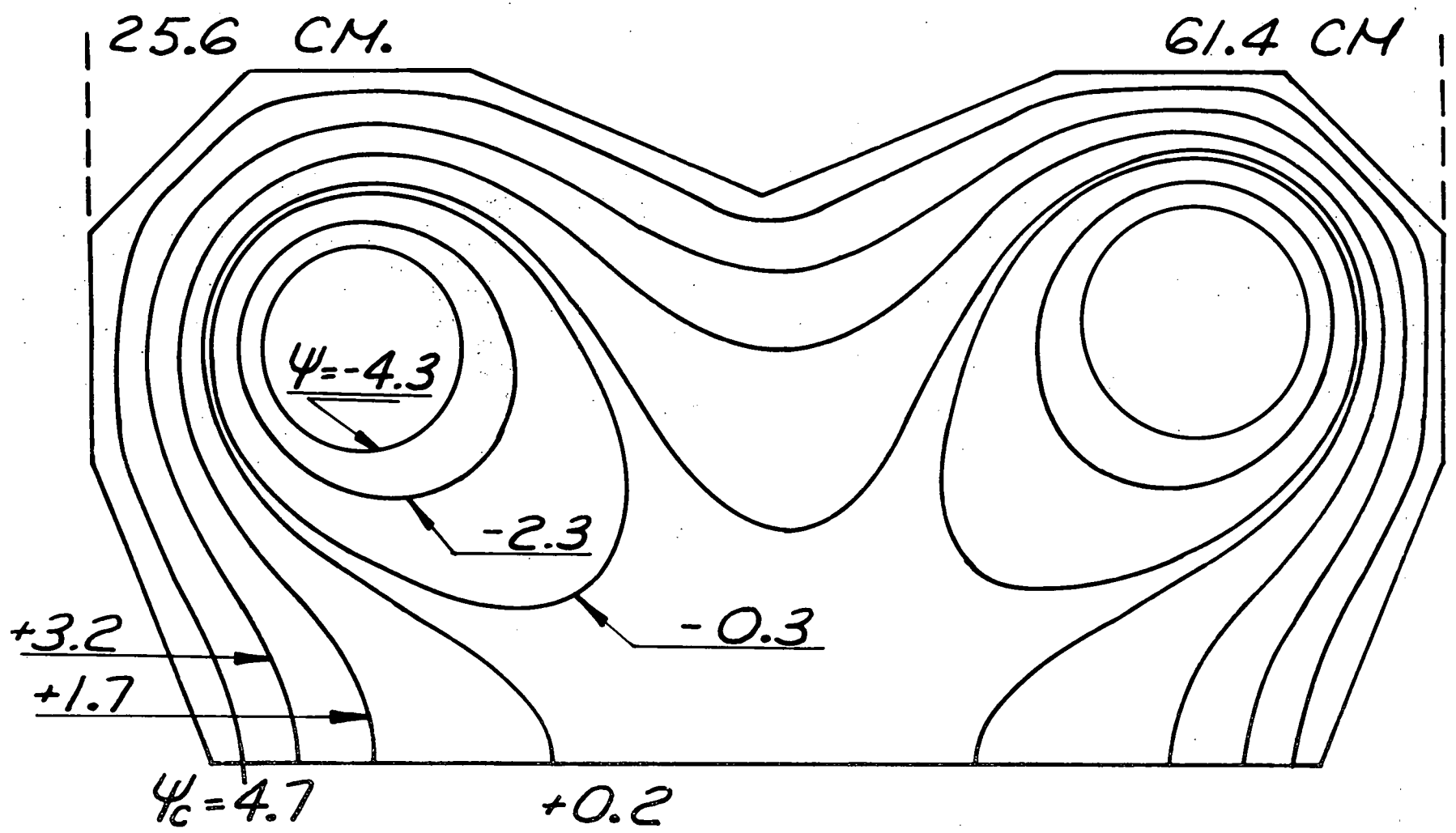

F. 3c

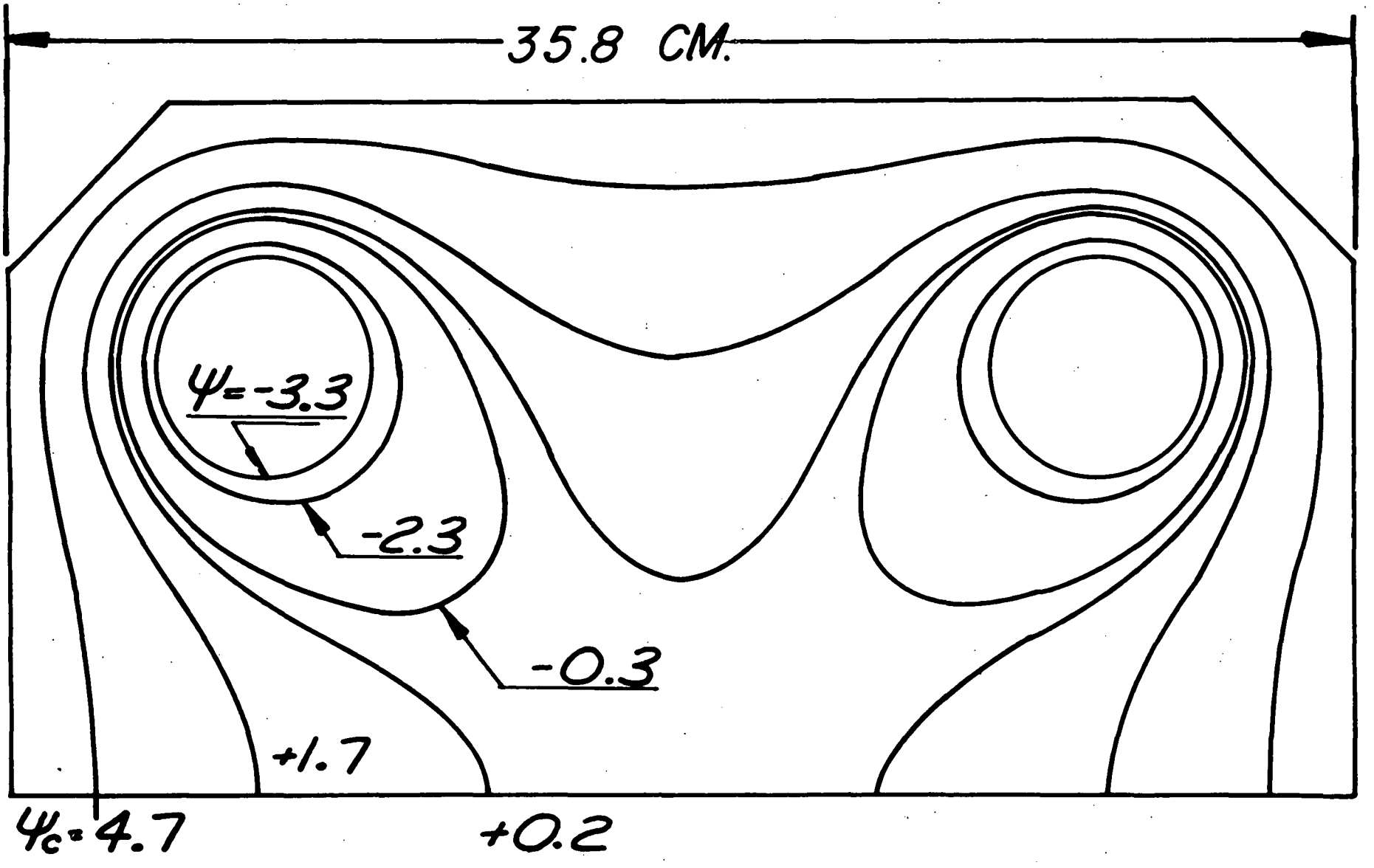
35.8 CM.
ψ=-3.3
-2.3
-0.3
+1.7
ψc=4.7
+0.2

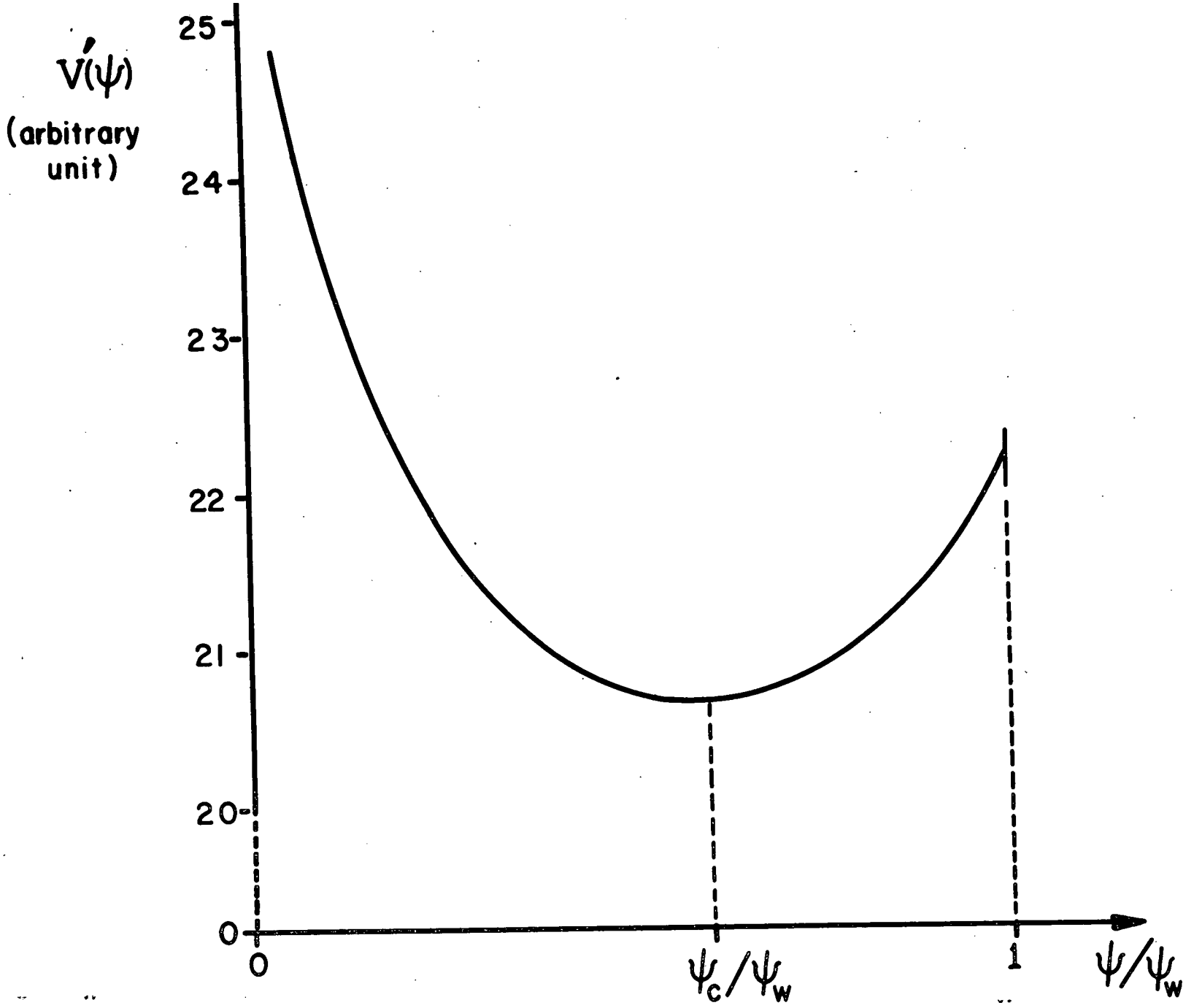
V'(ψ)
(arbitrary unit)
25
24
23
22
21
20
0
0
ψc/ψw
1
ψ/ψw

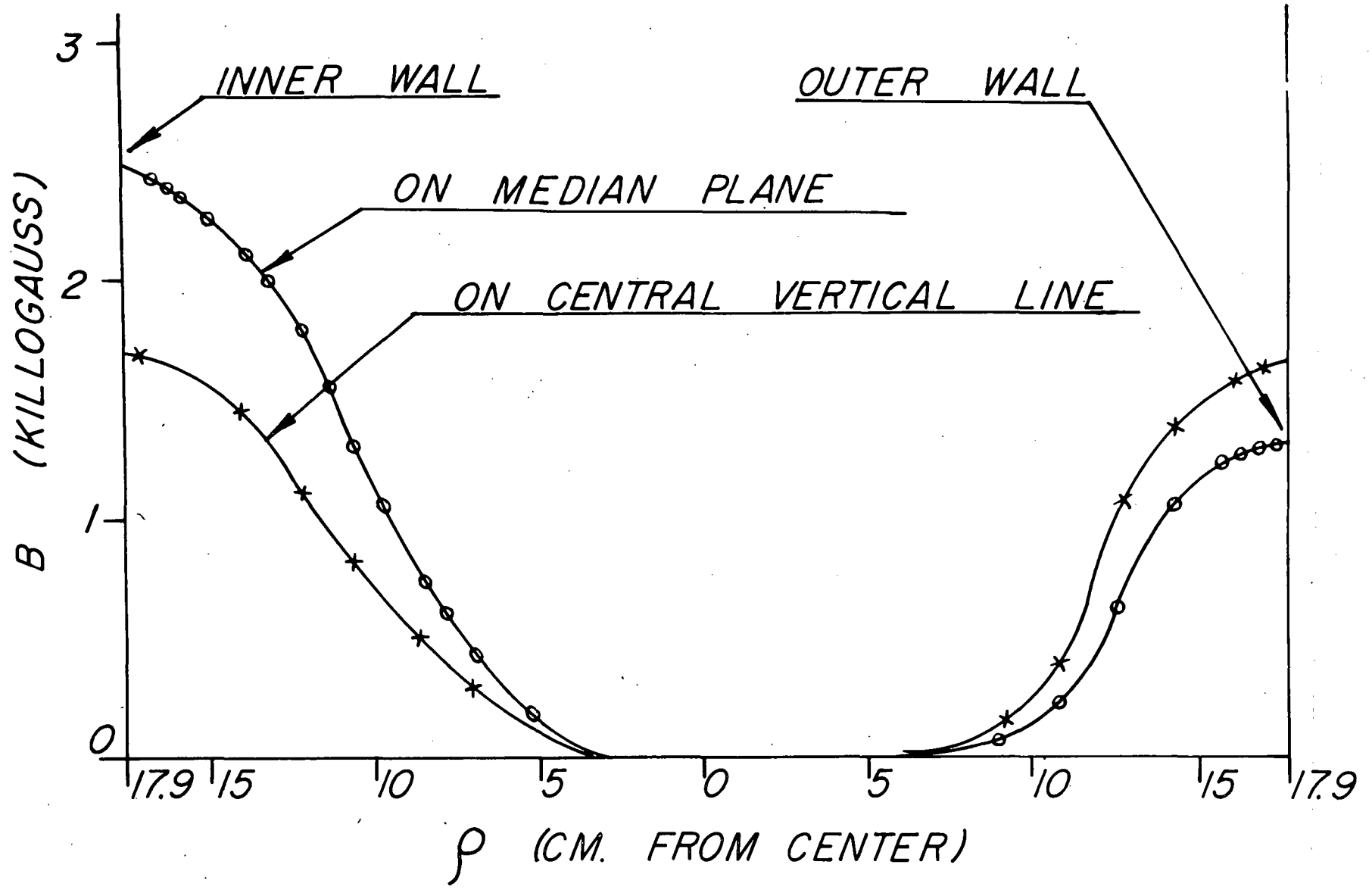
INNER WALL
OUTER WALL
ON MEDIAN PLANE
ON CENTRAL VERTICAL LINE
B (KILLOGAUSS)
3
2
1
0
17.9
15
10
5
0
5
10
15
17.9
ρ (CM. FROM CENTER)

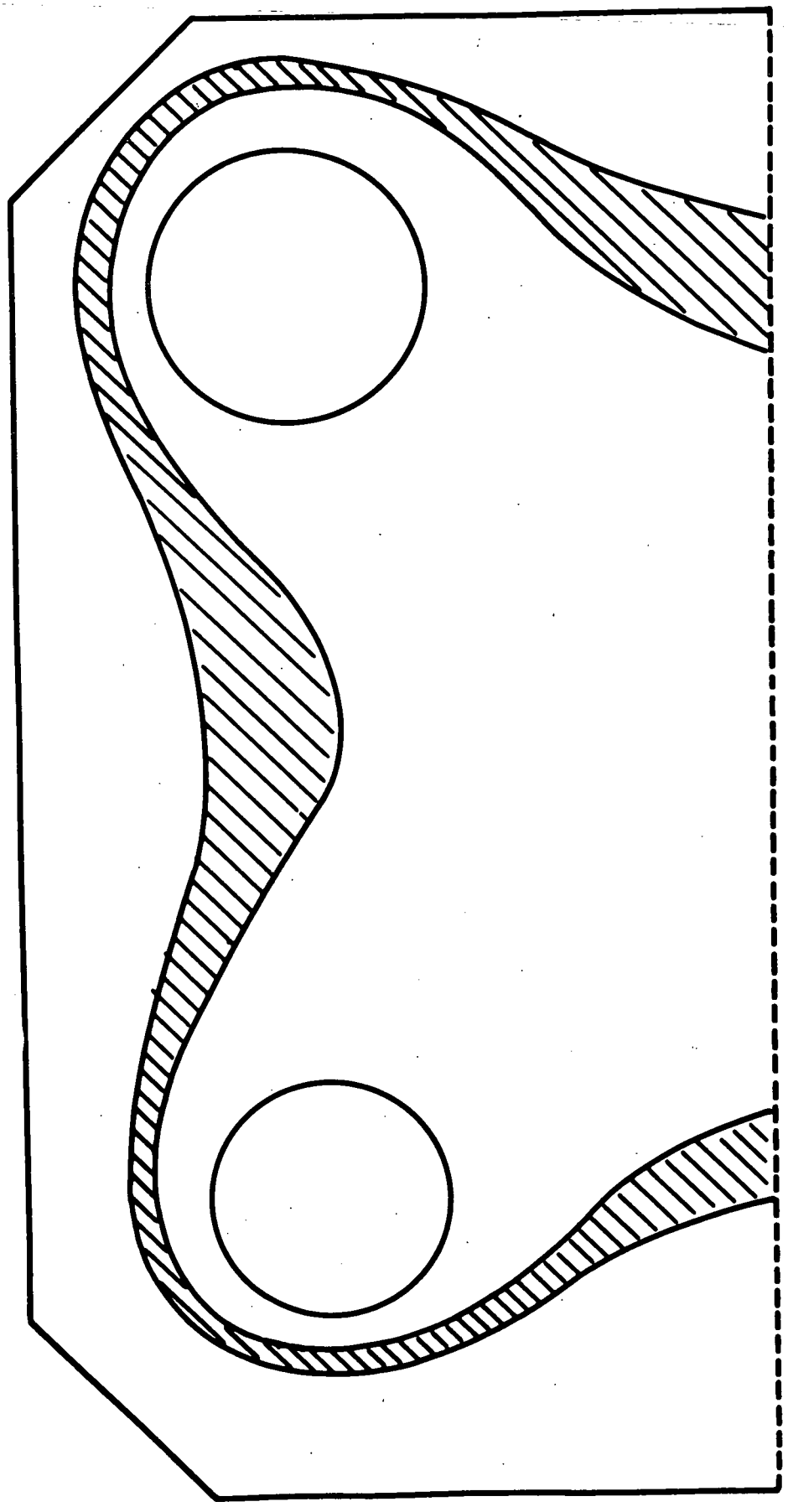

F. 6 A

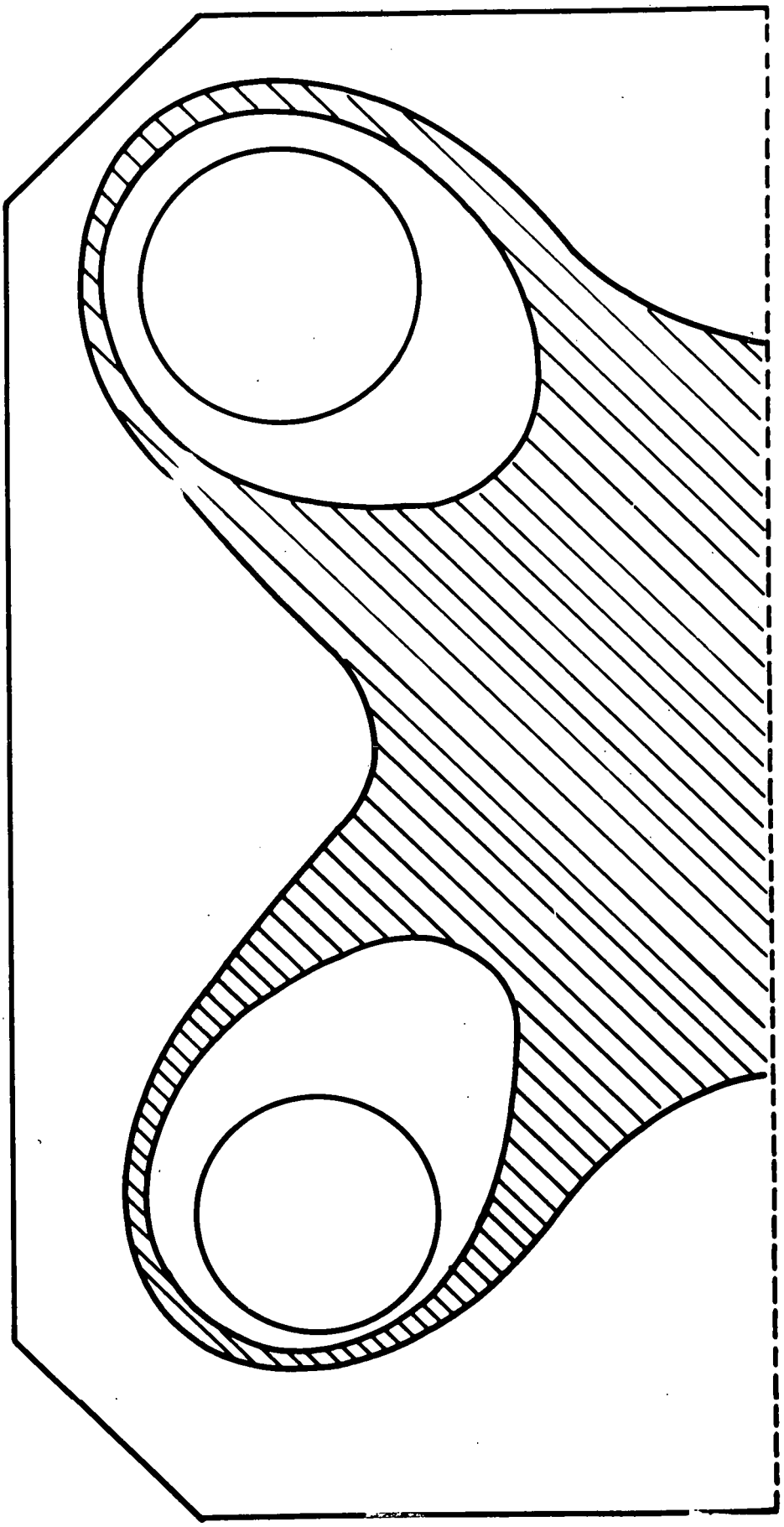

F 6B

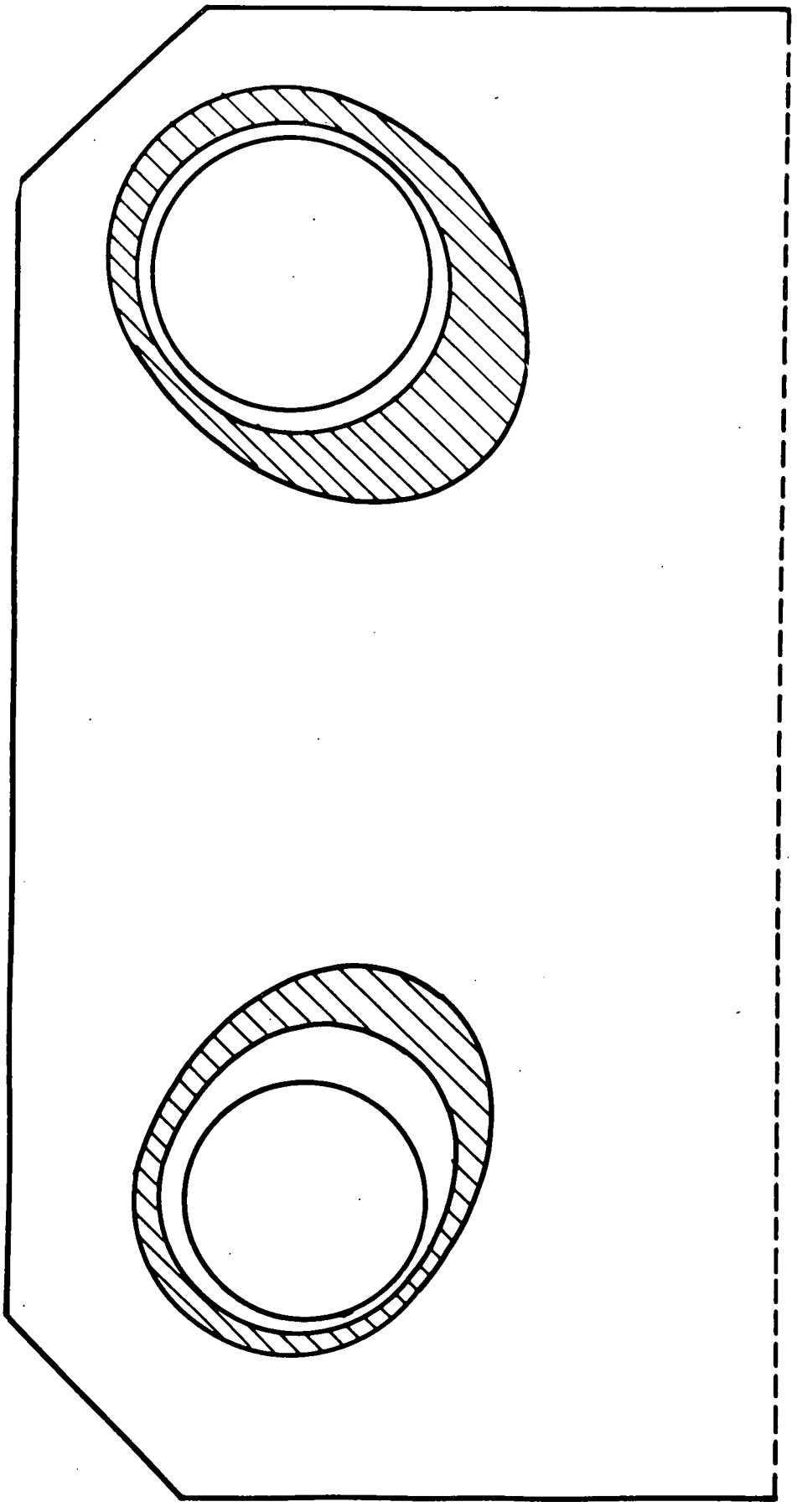

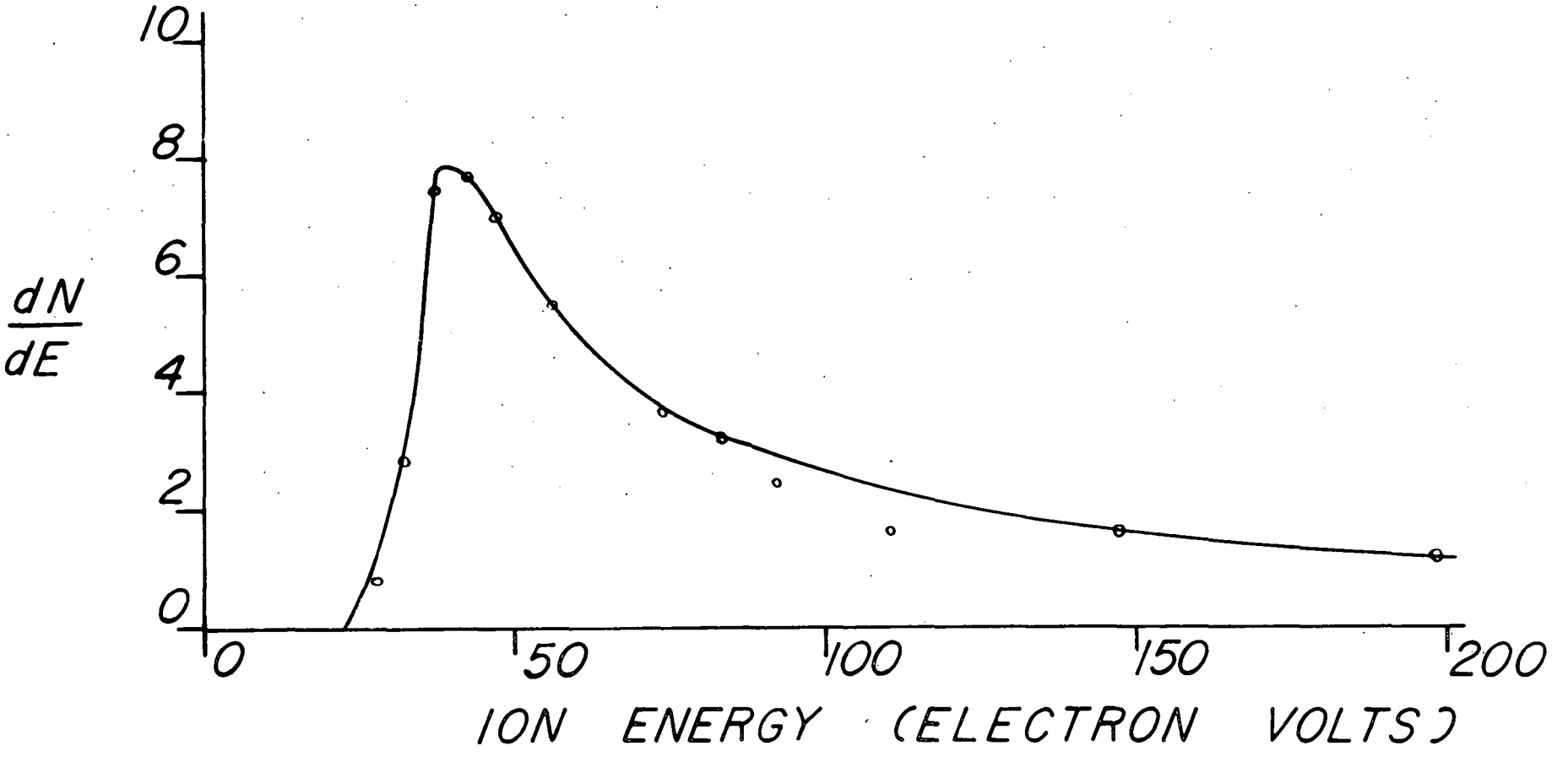
10
8
6
4
2
0
dN/dE
0
50
100
150
200
ION ENERGY (ELECTRON VOLTS)

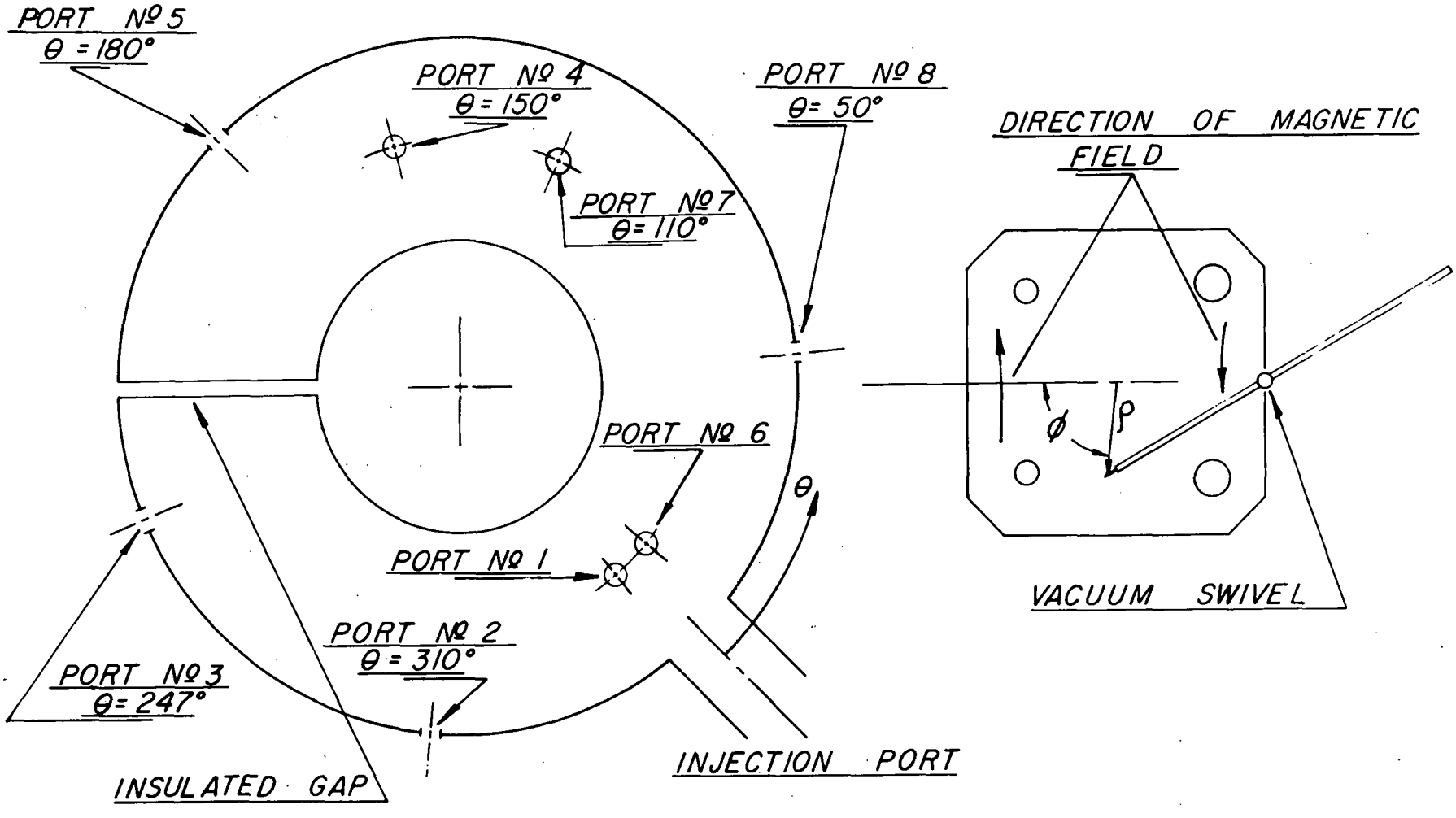
PORT Nº 5
θ = 180°
PORT Nº 4
θ = 150°
PORT Nº 8
θ = 50°
DIRECTION OF MAGNETIC FIELD
PORT Nº 7
θ = 110°
PORT Nº 6
θ
PORT Nº 1
VACUUM SWIVEL
PORT Nº 2
θ = 310°
PORT Nº 3
θ = 247°
INJECTION PORT
INSULATED GAP
ϕ
ρ

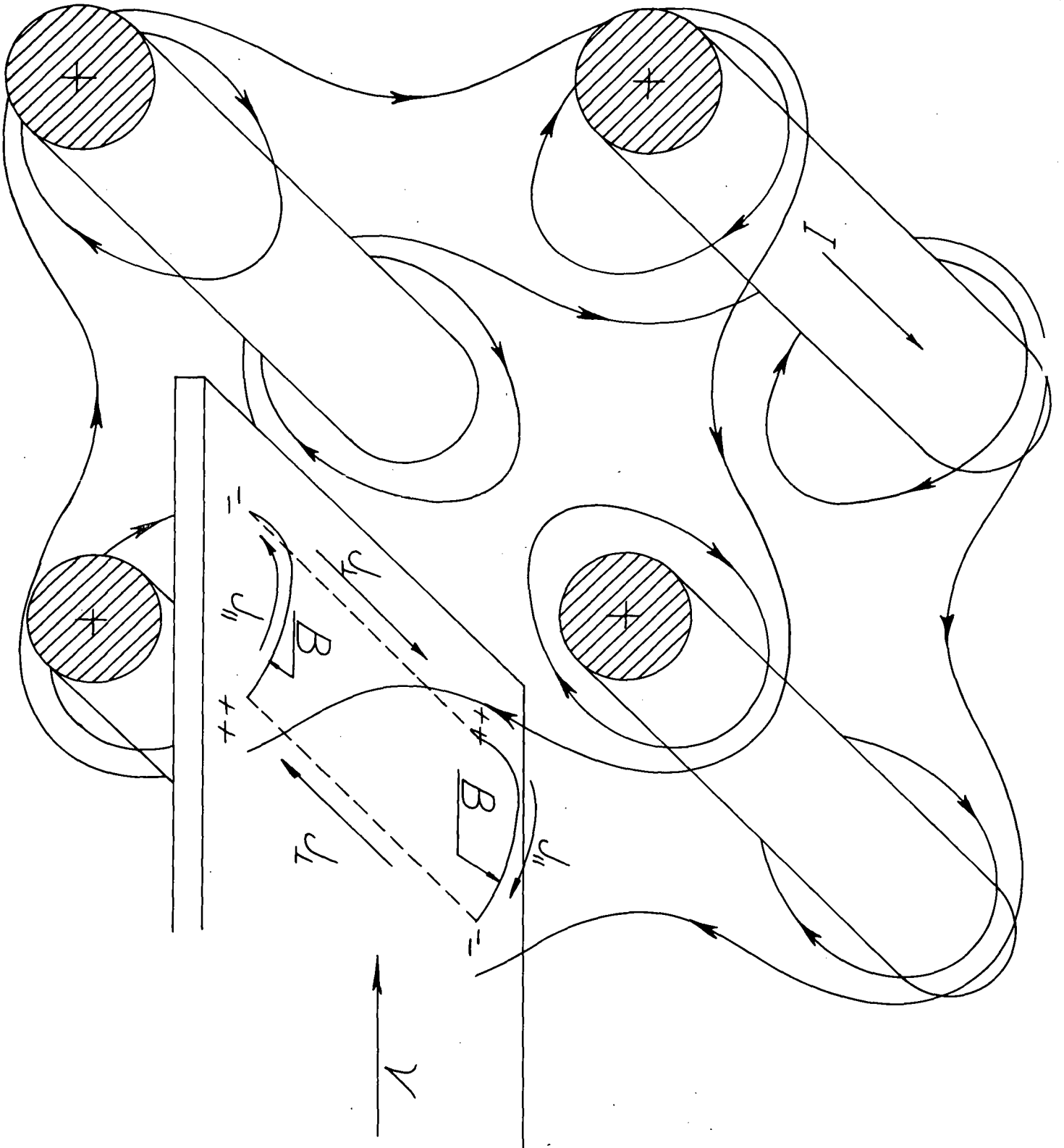
I
B
B
Y

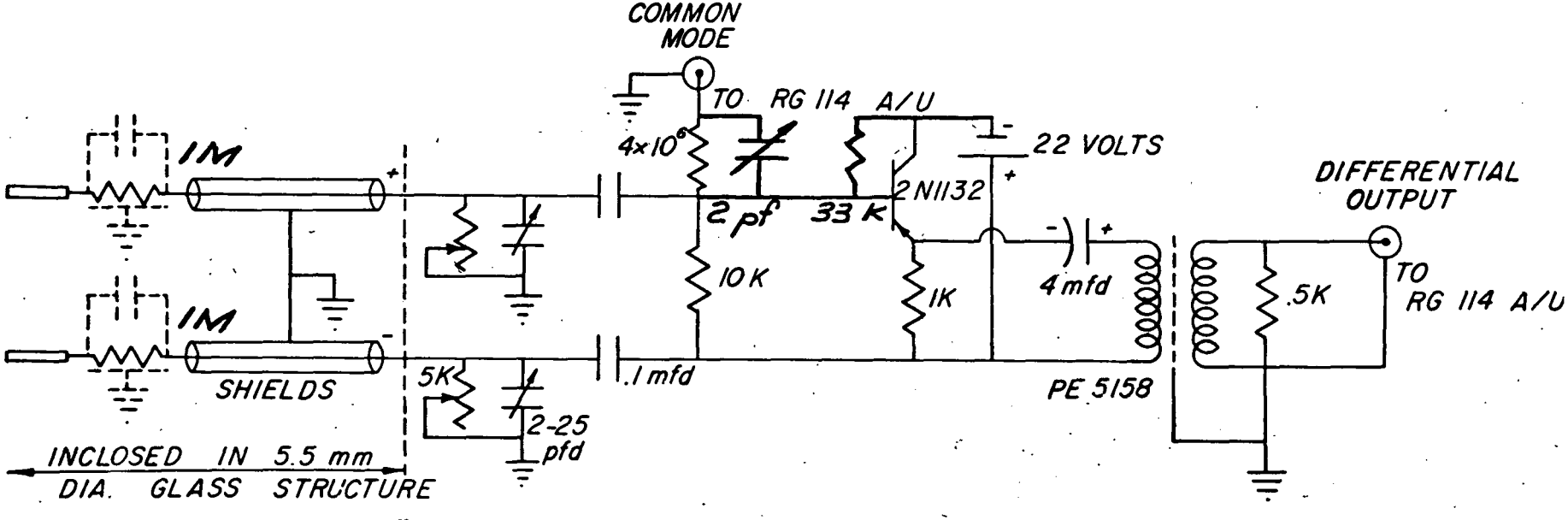
COMMON MODE
TO RG 114 A/U
4x10⁶
22 VOLTS
DIFFERENTIAL OUTPUT
IM
IM
2 pf
33 k
2N1132
10 K
1K
4 mfd
.5K
TO RG 114 A/U
SHIELDS
5K
2-25 pfd
.1 mfd
PE 5158
INCLOSED IN 5.5 mm DIA. GLASS STRUCTURE

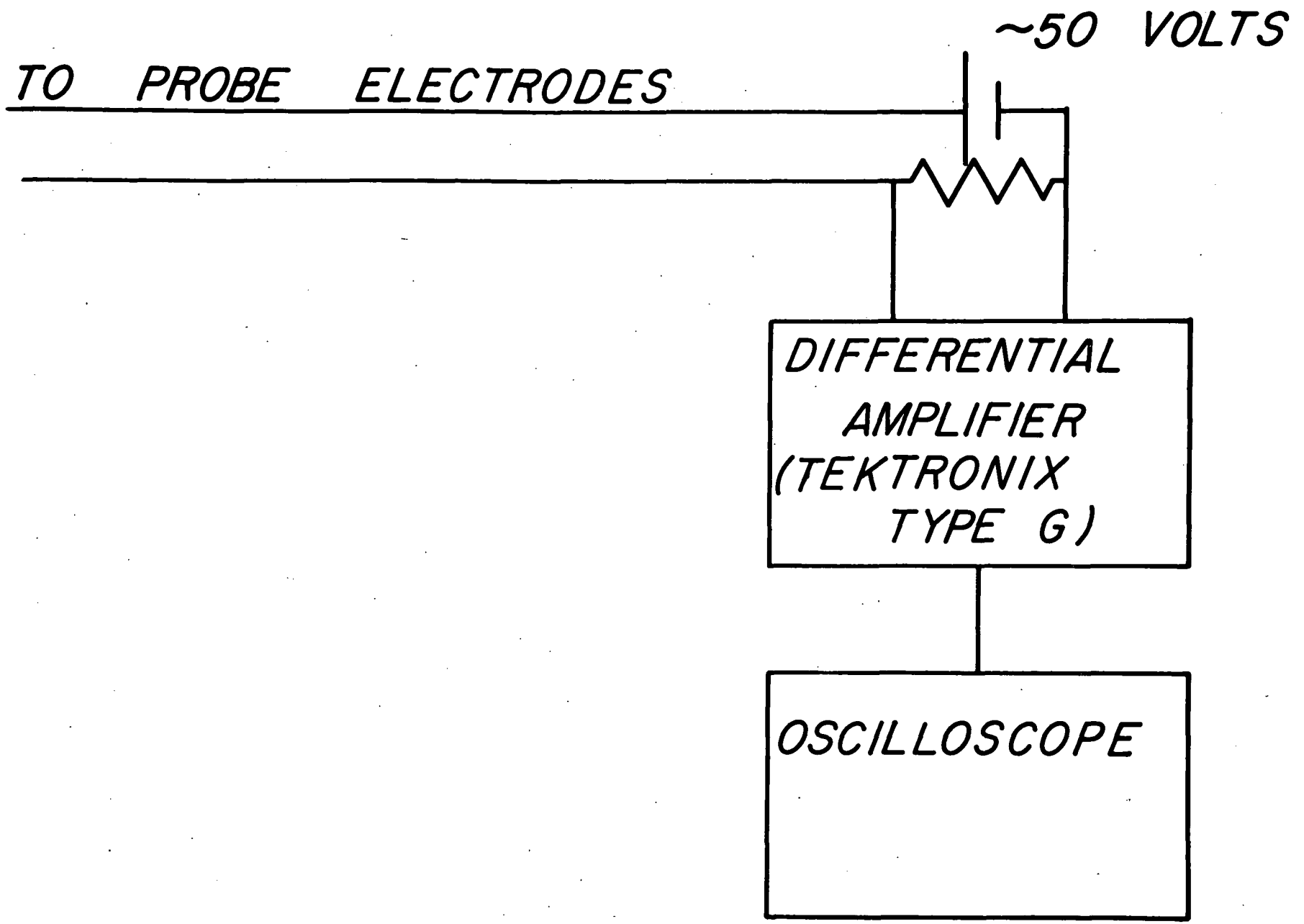
~50 VOLTS
TO PROBE ELECTRODES
DIFFERENTIAL AMPLIFIER (TEKTRONIX TYPE G)
OSCILLOSCOPE

Fig 1

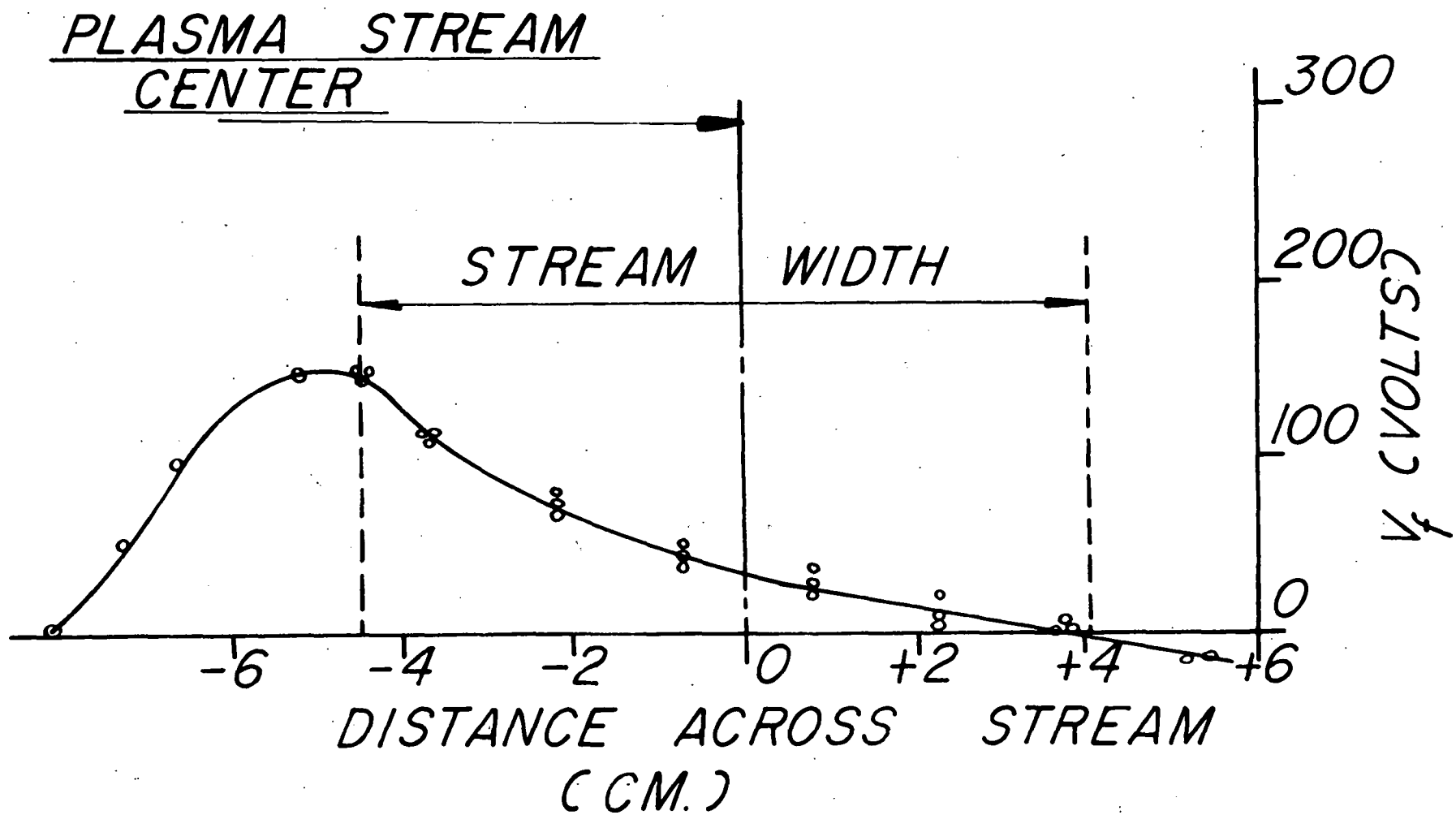
PLASMA STREAM CENTER
STREAM WIDTH
300
200
100
0
V_f (VOLTS)
-6
-4
-2
0
+2
+4
+6
DISTANCE ACROSS STREAM
(CM.)

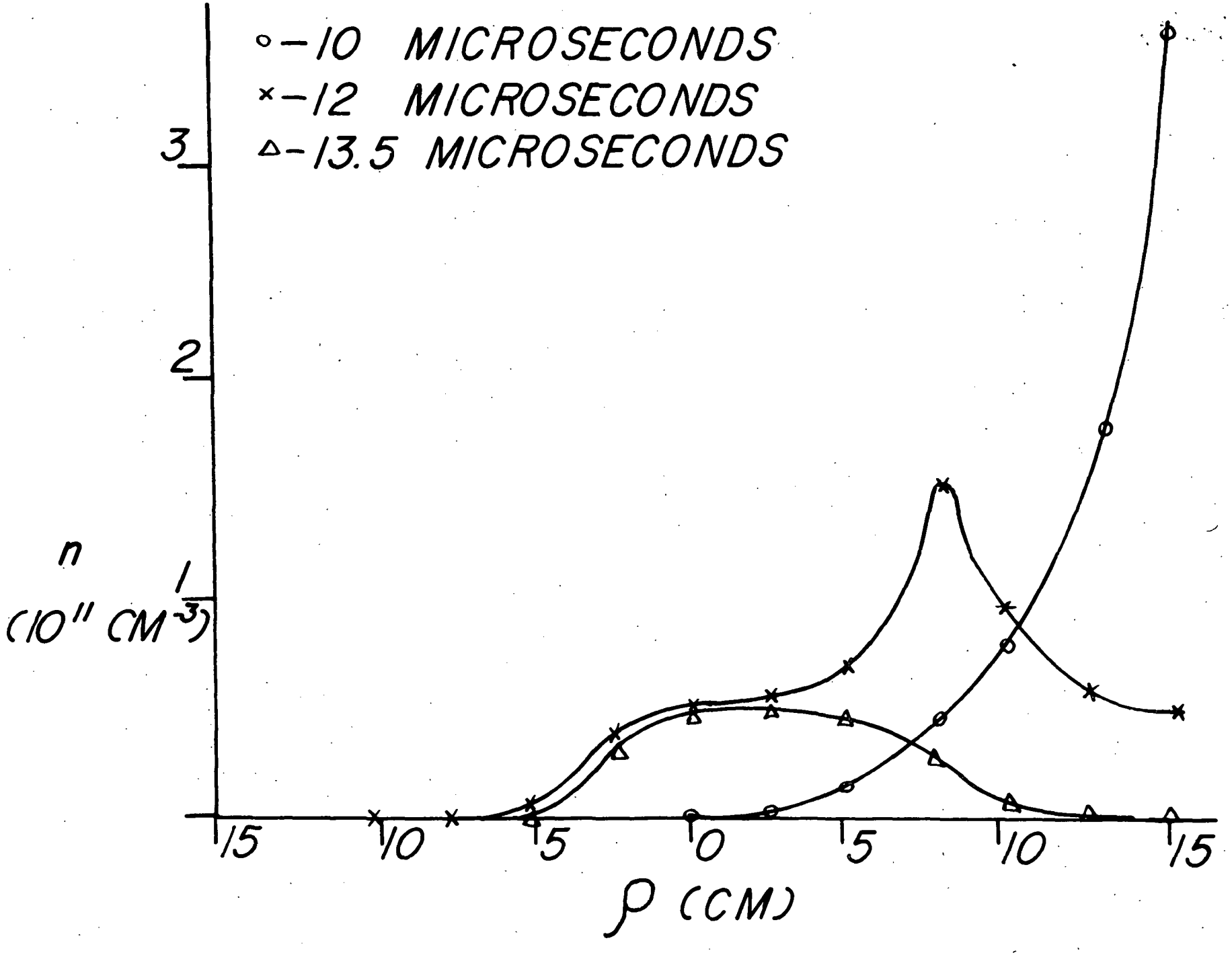
o - 10 MICROSECONDS
× - 12 MICROSECONDS
Δ - 13.5 MICROSECONDS
3
2
1
n
(10^11 CM^-3)
15
10
5
0
5
10
15
ρ (CM)

F12

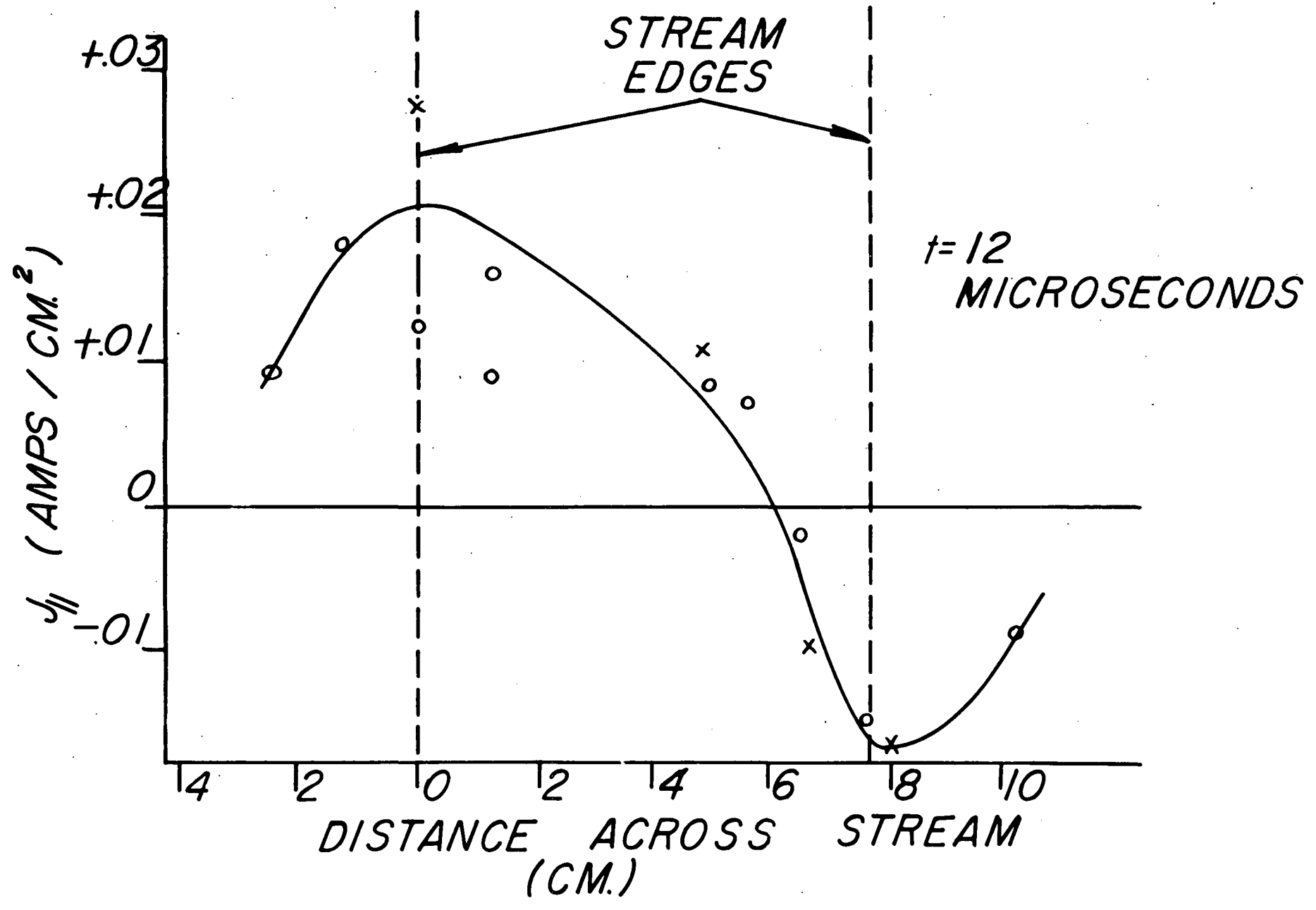
STREAM
EDGES
t= 12
MICROSECONDS
+.03
+.02
+.01
0
-.01
$J_{//}$ (AMPS / CM.^{2})
4
2
0
2
4
6
8
10
DISTANCE ACROSS STREAM
(CM.)

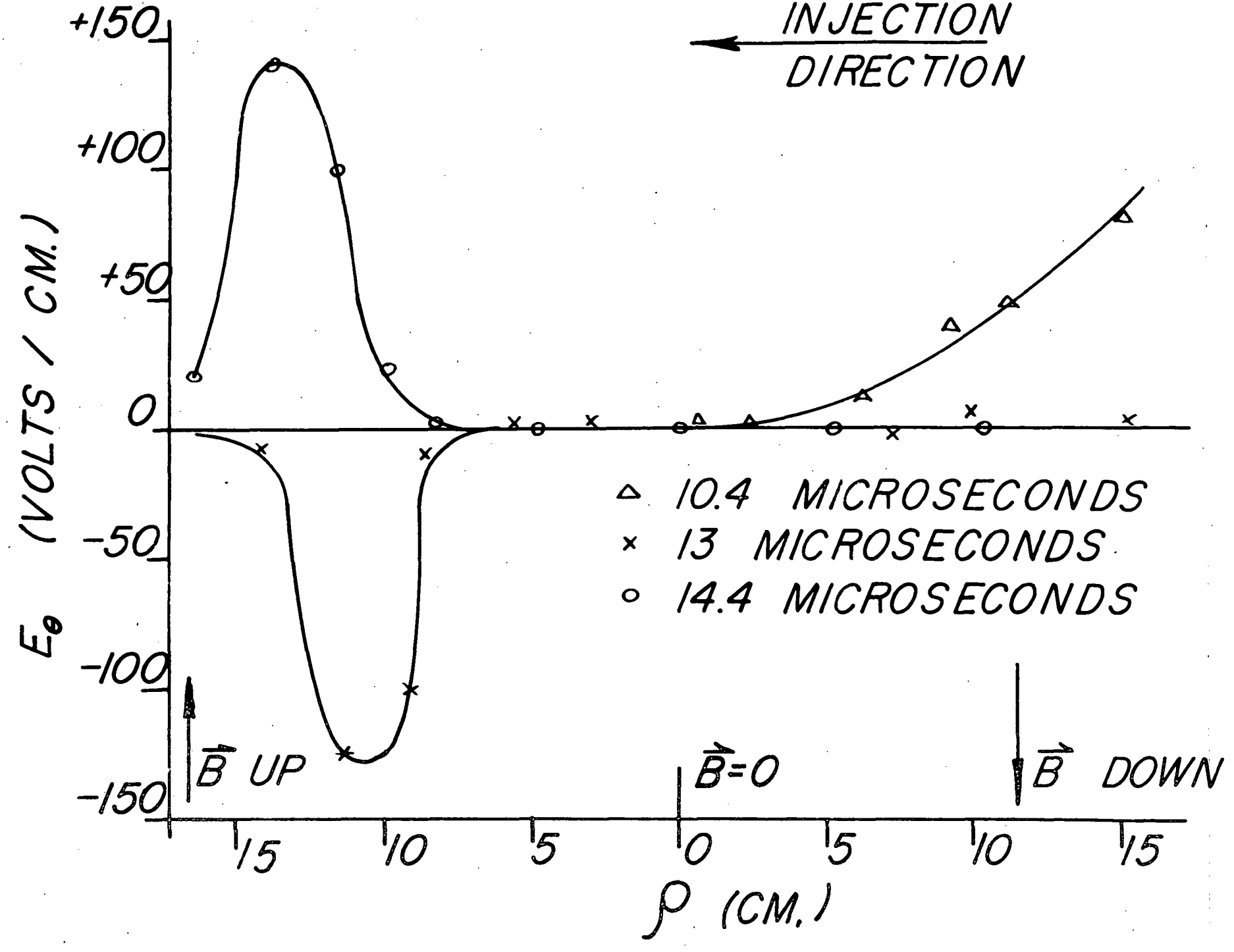
INJECTION DIRECTION
+150
+100
+50
0
-50
-100
-150
E_θ (VOLTS / CM.)
△ 10.4 MICROSECONDS
× 13 MICROSECONDS
○ 14.4 MICROSECONDS
$\vec{B}$ UP
$\vec{B}$=0
$\vec{B}$ DOWN
15
10
5
0
5
10
15
ρ (CM.)

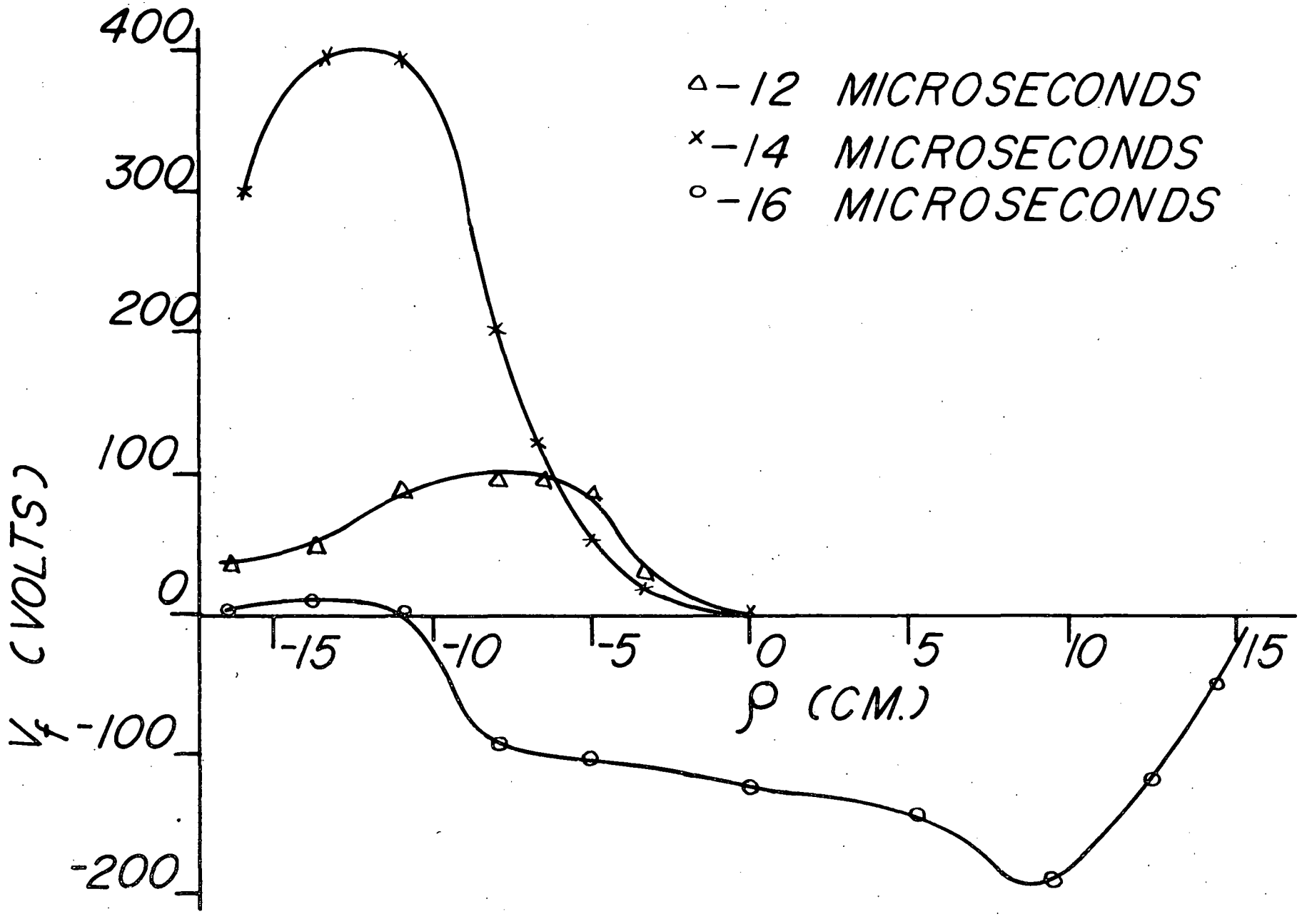
400
300
200
100
0
-100
-200
V_f (VOLTS)
-15
-10
-5
0
5
10
15
ρ (CM.)
△ - 12 MICROSECONDS
× - 14 MICROSECONDS
○ - 16 MICROSECONDS

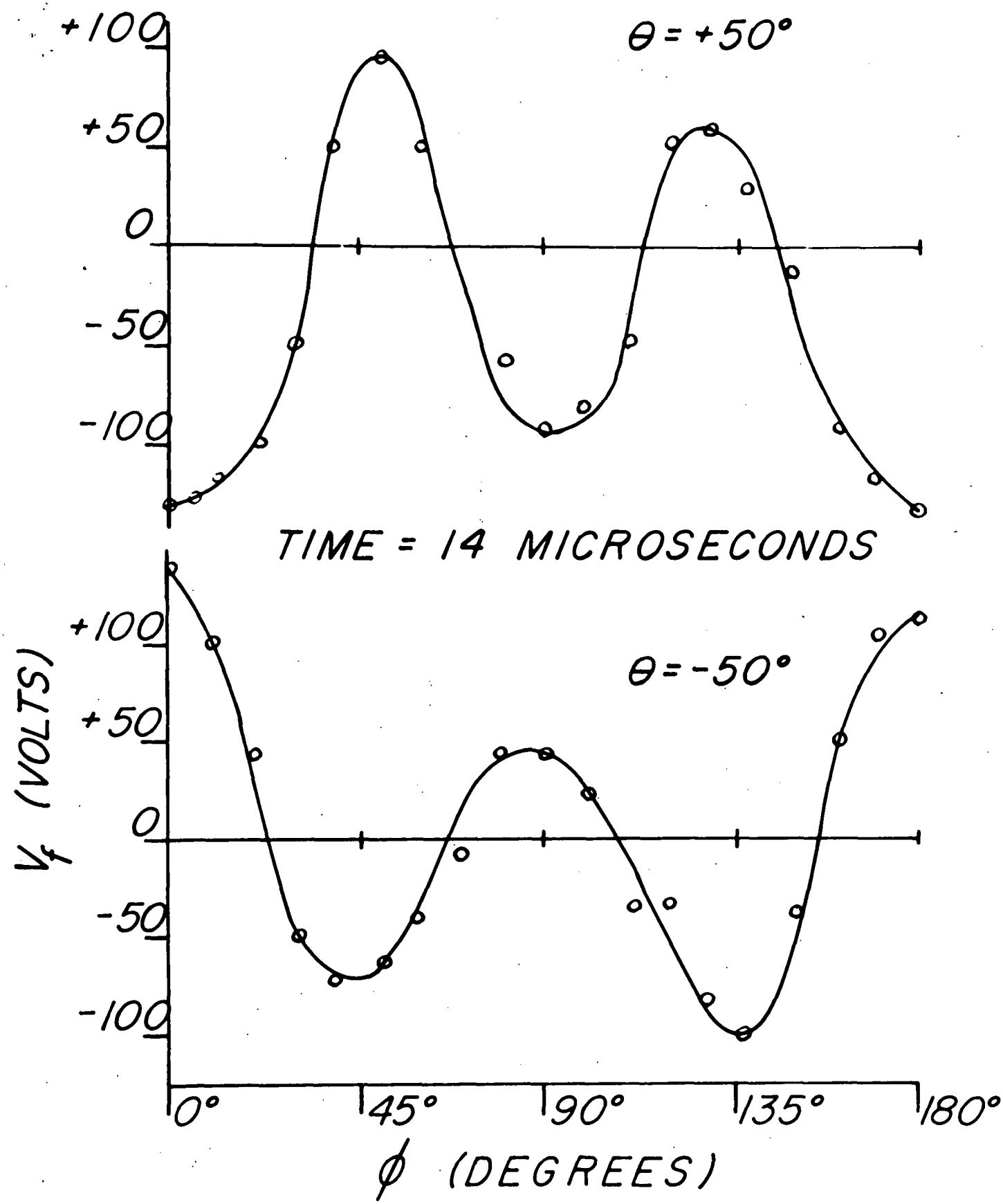
+100
+50
0
-50
-100
θ = +50°
TIME = 14 MICROSECONDS
+100
+50
0
-50
-100
θ = -50°
V_f (VOLTS)
0°
45°
90°
135°
180°
φ (DEGREES)

Fig 17

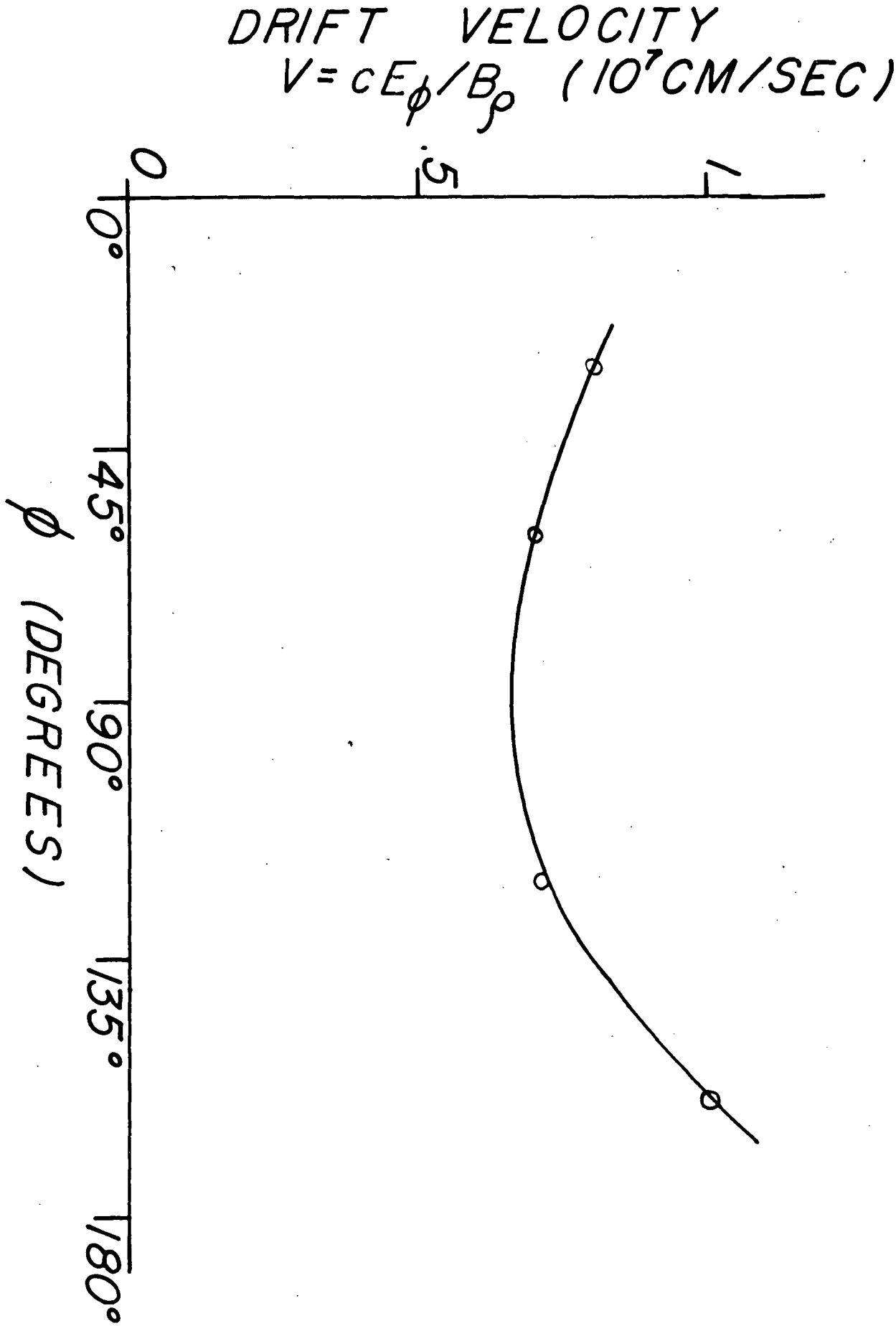

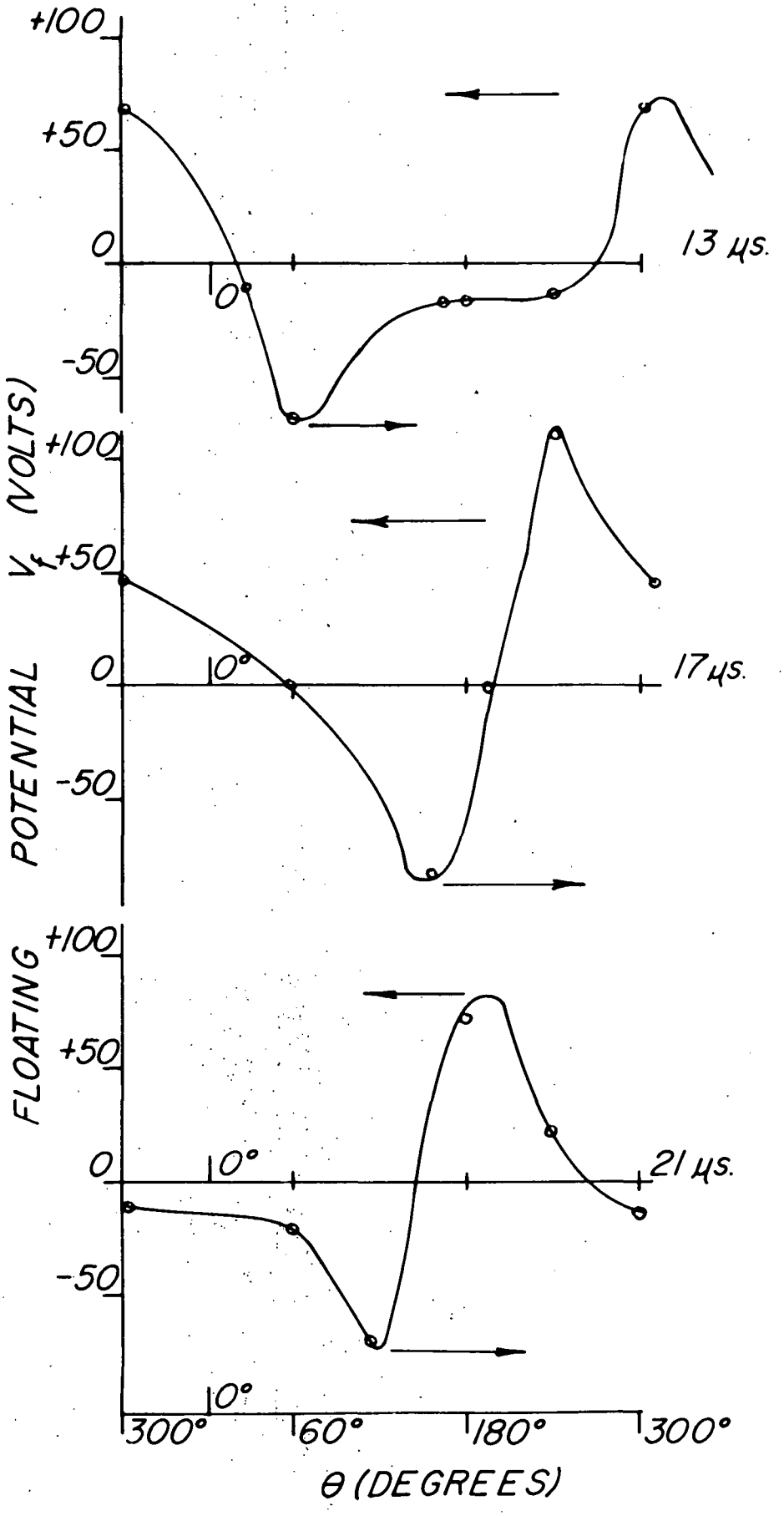
+100
+50
0
-50
13 μs.
0°
+100
+50
0
-50
17 μs.
0°
+100
+50
0
-50
21 μs.
0°
0°
300°
60°
180°
300°
θ (DEGREES)
FLOATING POTENTIAL V_f (VOLTS)

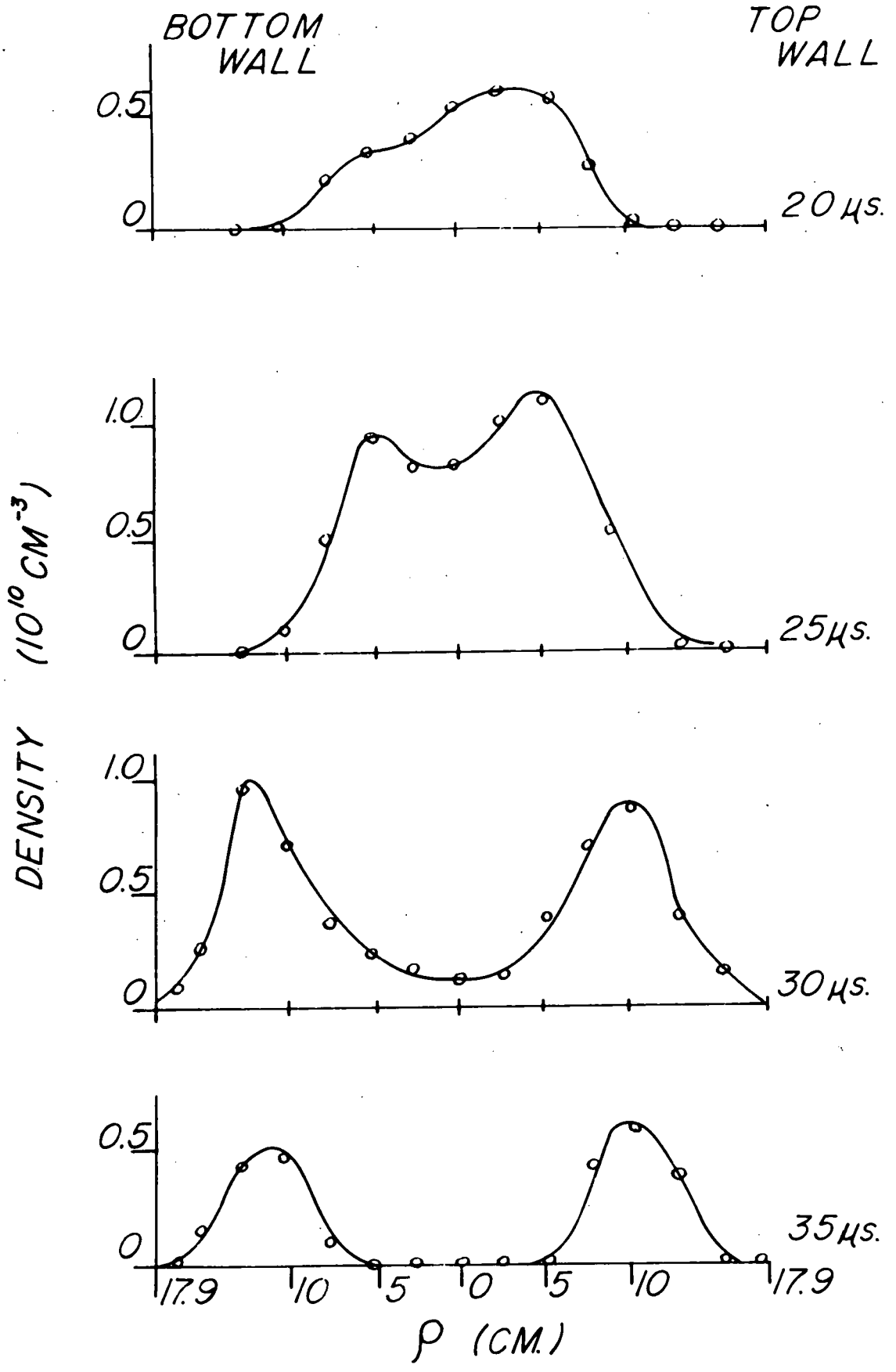
BOTTOM WALL
TOP WALL
0.5
0
20 μs.
1.0
0.5
0
25μs.
DENSITY (10^10 CM^-3)
1.0
0.5
0
30 μs.
0.5
0
35μs.
17.9
10
5
0
5
10
17.9
ρ (CM.)

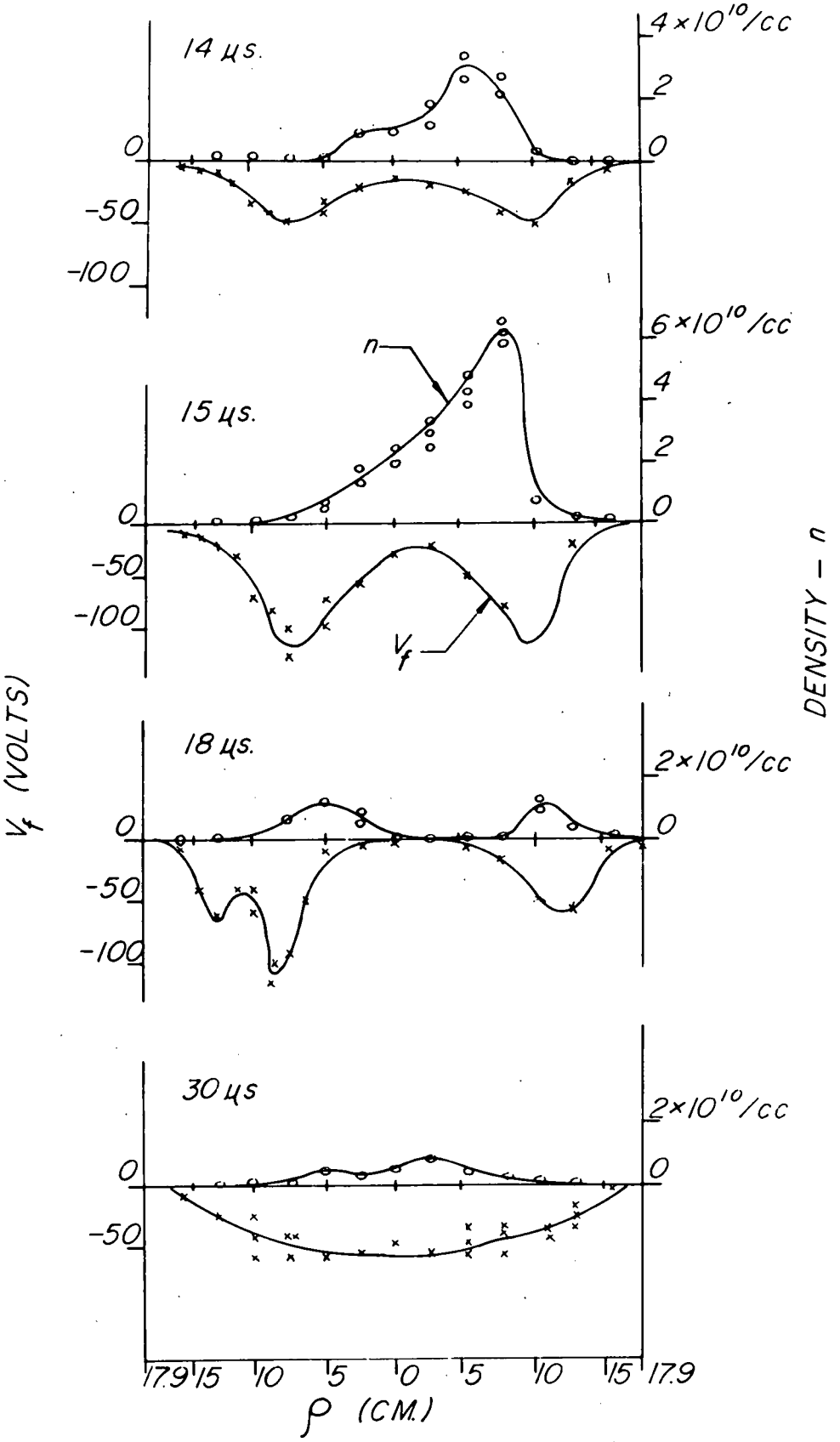
14 μs.
4×10^10/cc
2
0
0
-50
-100
n
15 μs.
6×10^10/cc
4
2
0
0
-50
-100
V_f
18 μs.
2×10^10/cc
0
0
-50
-100
30 μs
2×10^10/cc
0
0
-50
17.9 15 10 5 0 5 10 15 17.9
ρ (CM.)
V_f (VOLTS)
DENSITY – n

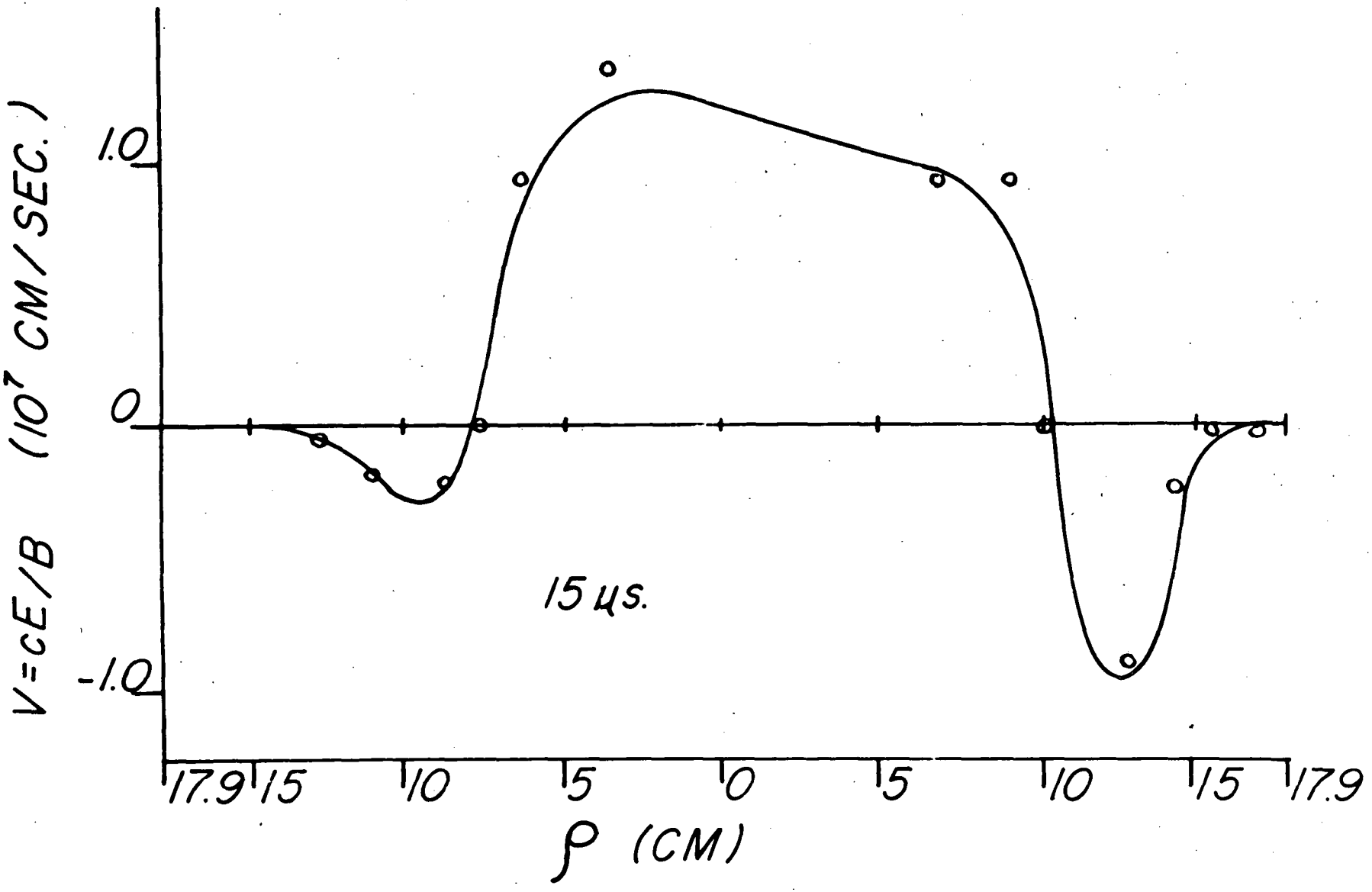

Fig 21

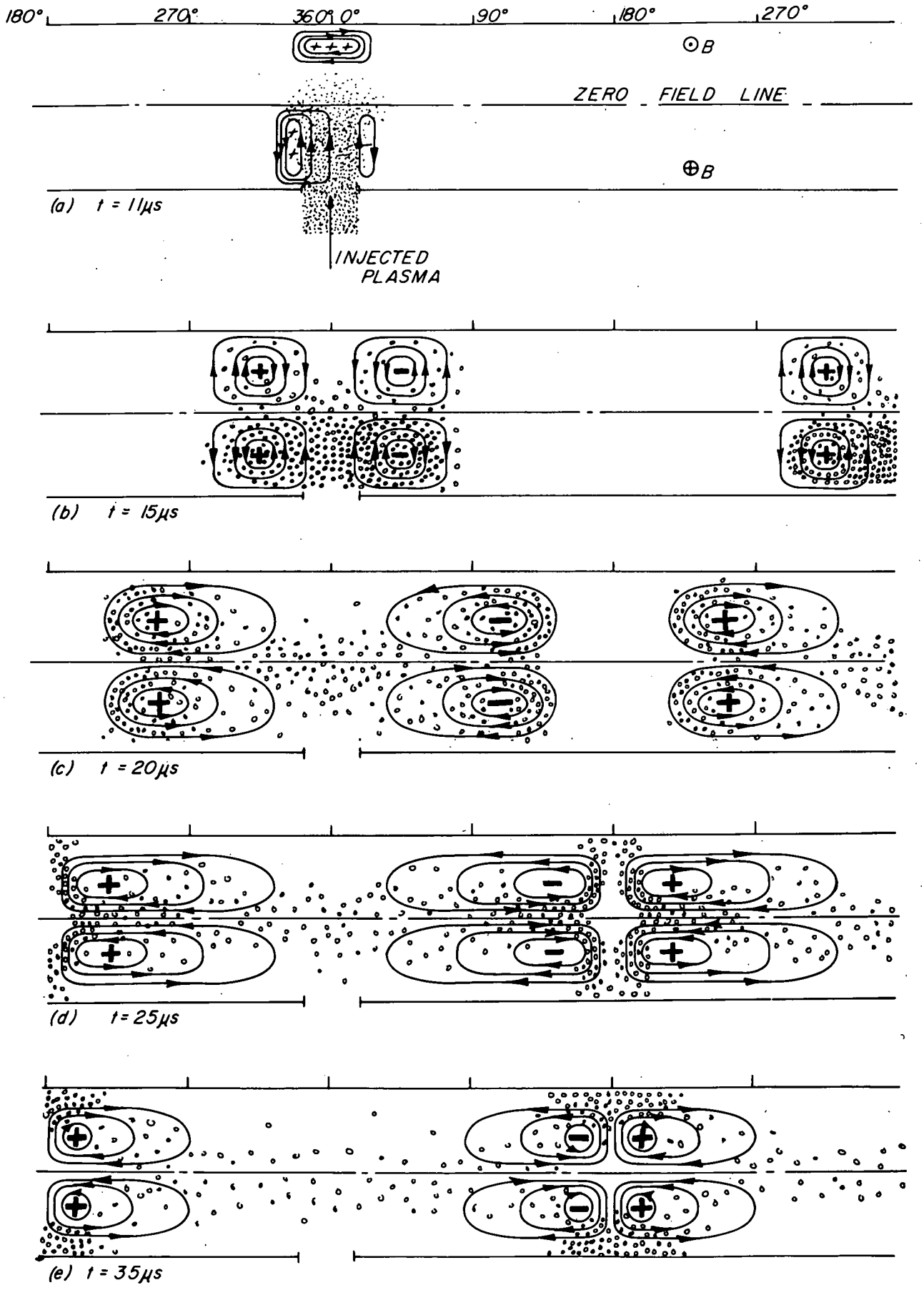
180°
270°
360° 0°
90°
180°
270°
⊙B
ZERO FIELD LINE
⊕B
(a) t = 11μs
INJECTED PLASMA
(b) t = 15μs
(c) t = 20μs
(d) t = 25μs
(e) t = 35μs

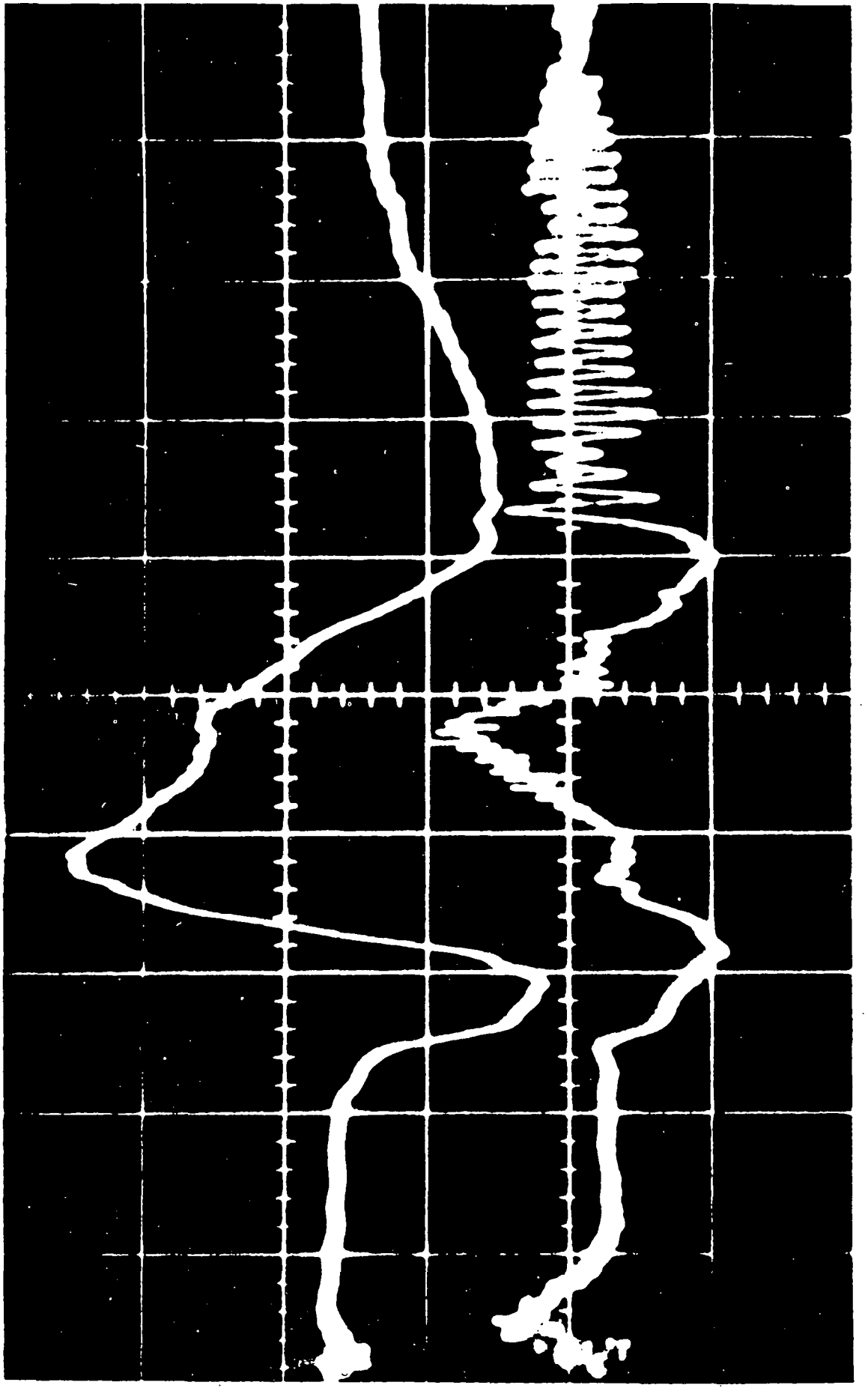

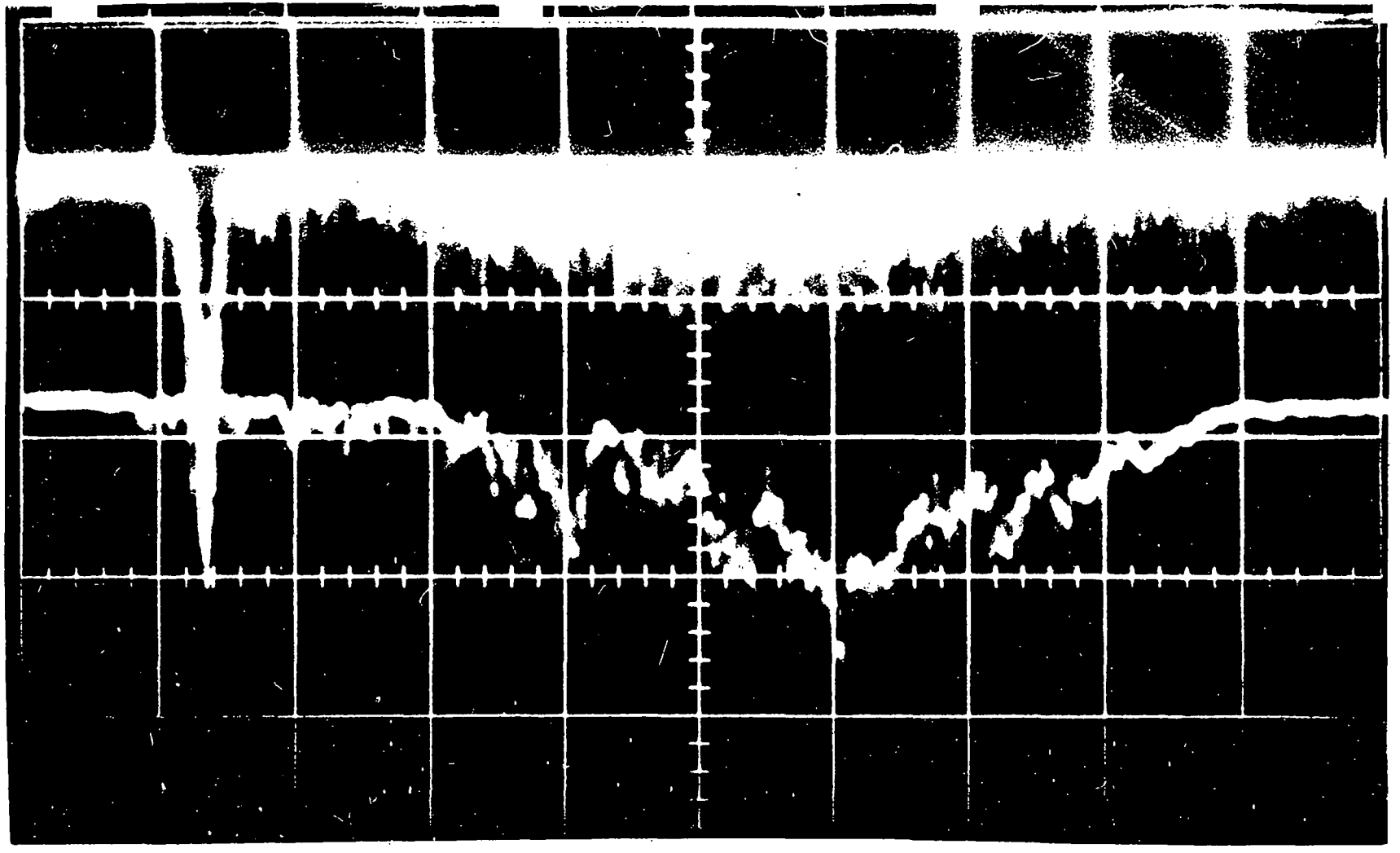

20 μs/cm.

Fig.25

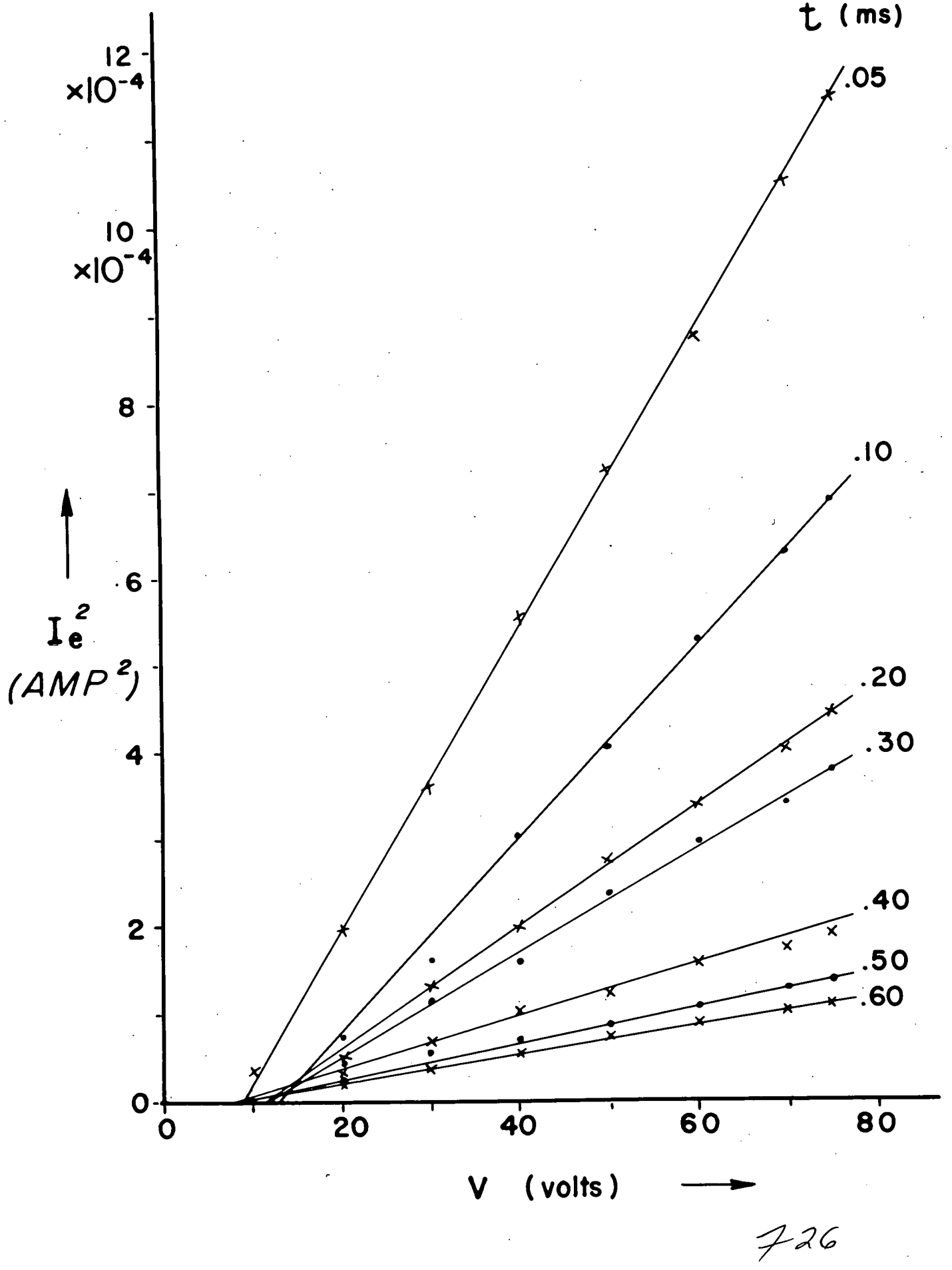
t (ms)
.05
.10
.20
.30
.40
.50
.60
12 ×10⁻⁴
10 ×10⁻⁴
8
6
4
2
0
I_e^2 (AMP²)
0
20
40
60
80
V (volts)

F26

Multipole

Primary
Current

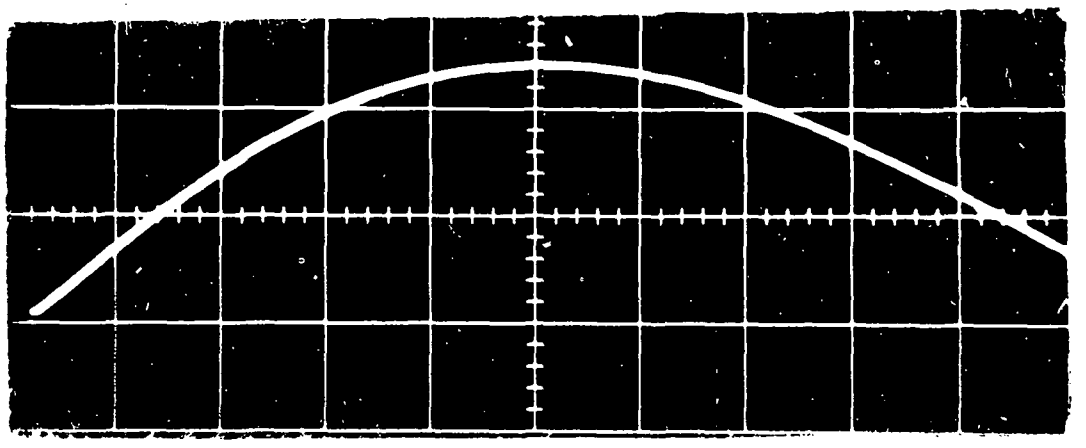

Output
Detector

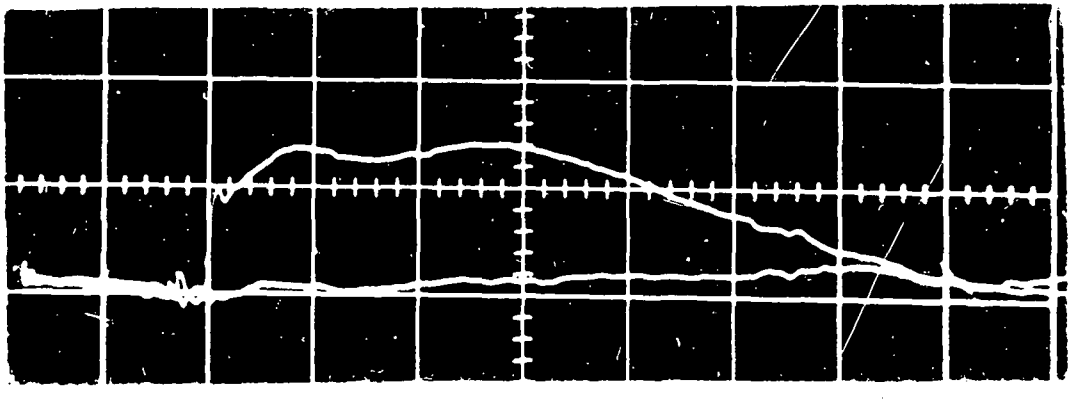

t ⟶

(0.5ms/cm)

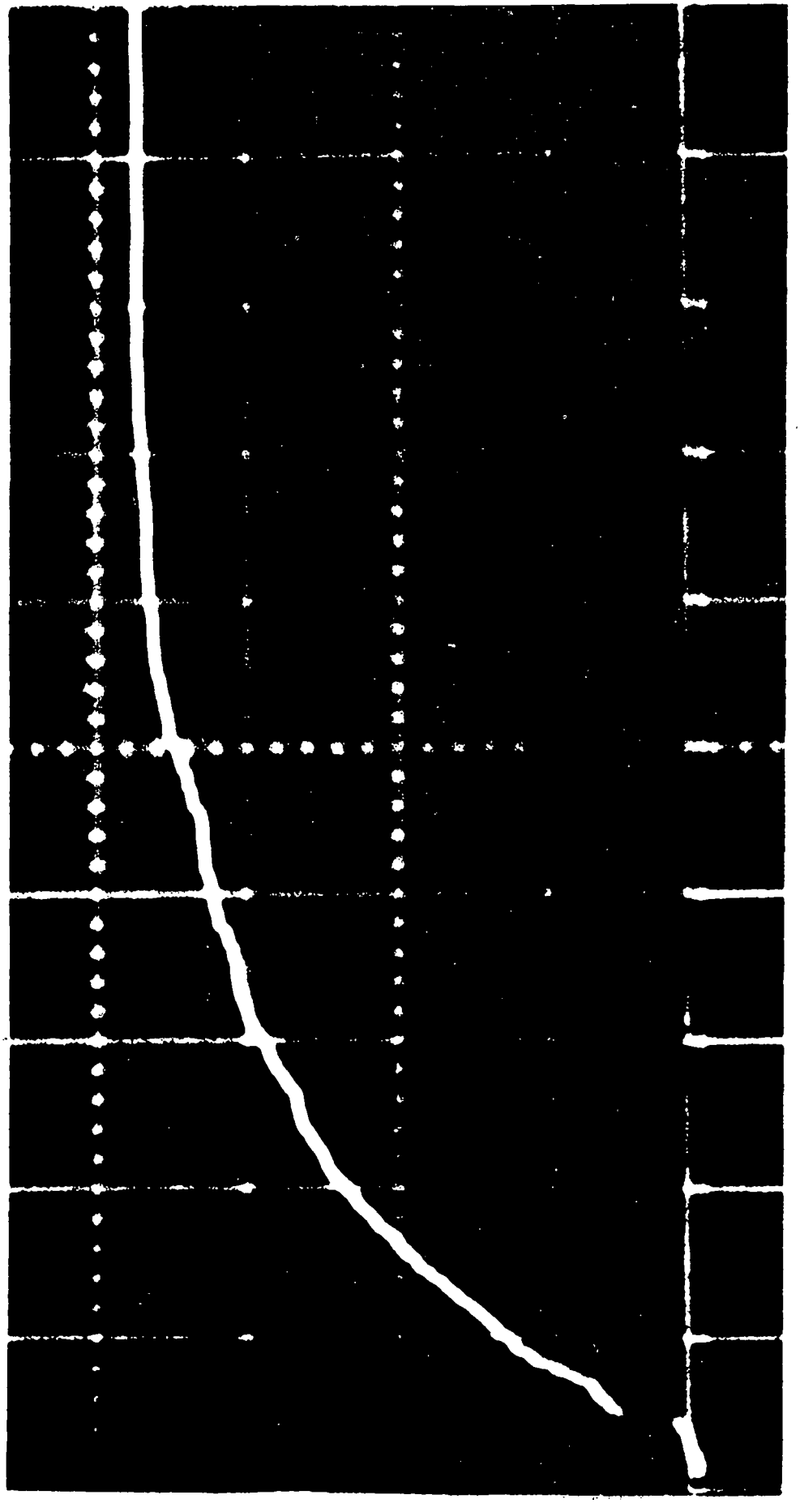

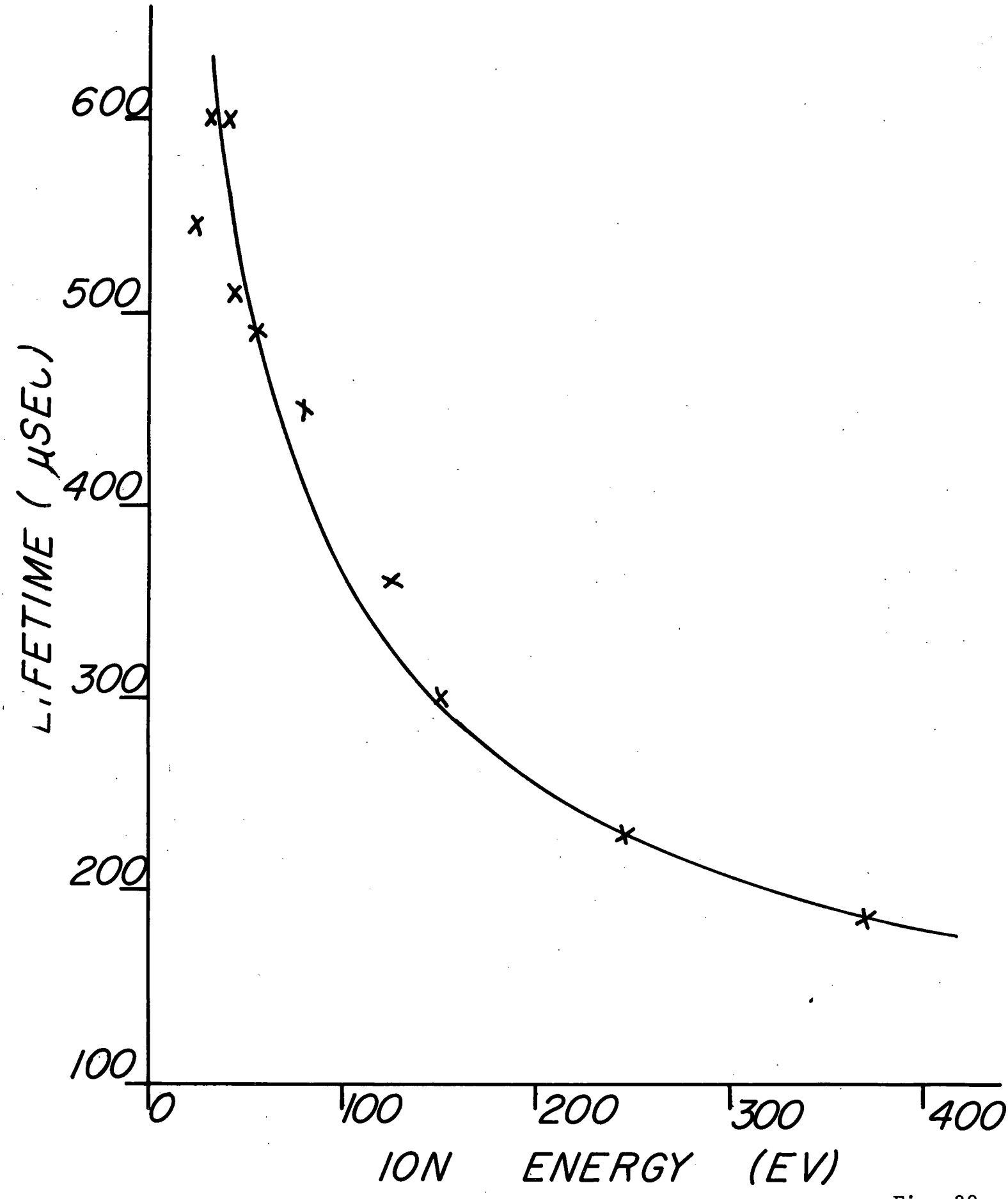
600
500
400
300
200
100
LIFETIME (μSEC)
0
100
200
300
400
ION ENERGY (EV)

Fig. 29

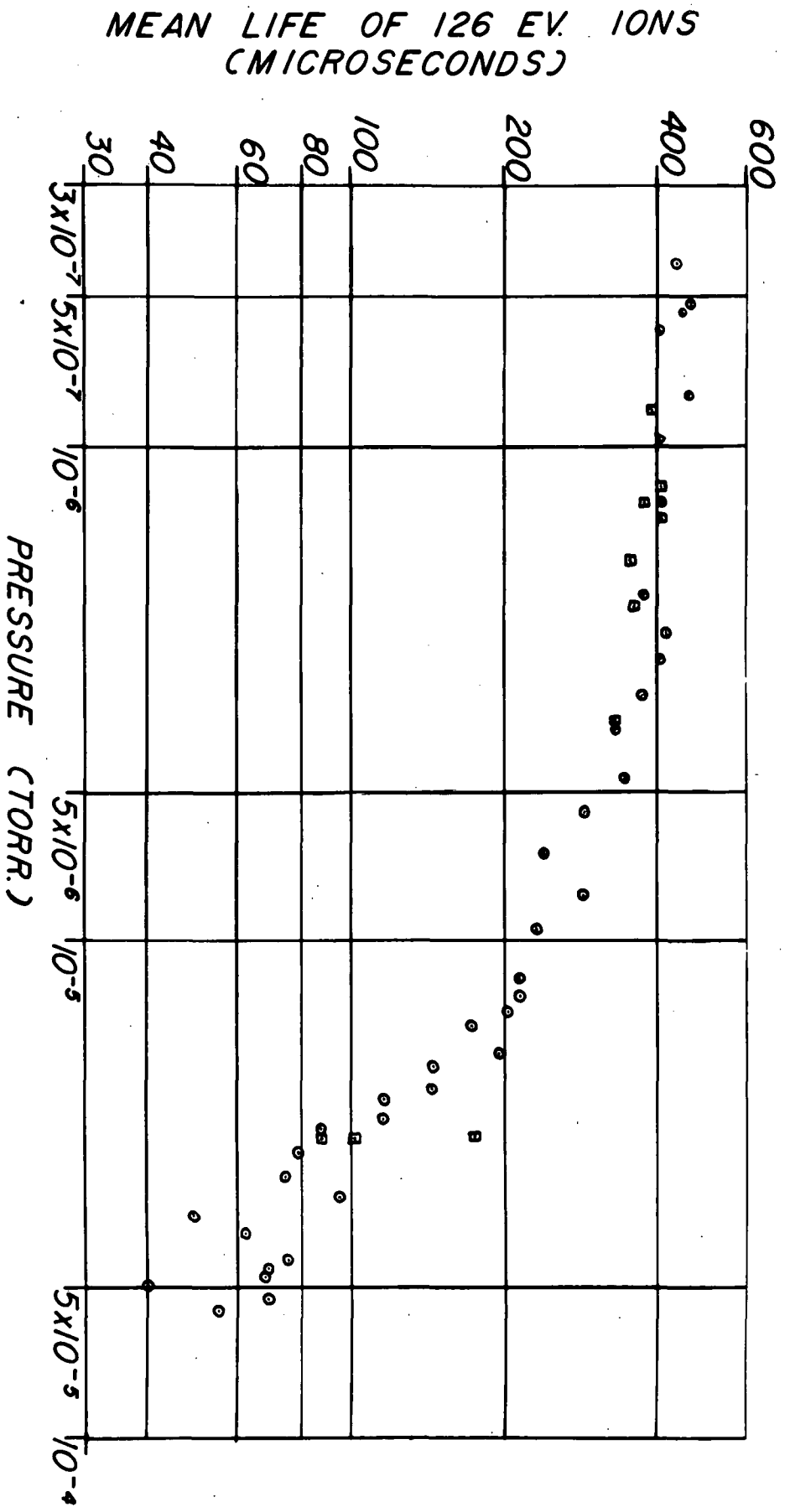
MEAN LIFE OF 126 EV. IONS
(MICROSECONDS)
30
40
60
80
100
200
400
600
3x10⁻⁷
5x10⁻⁷
1/0⁻⁶
5x10⁻⁶
1/0⁻⁵
5x10⁻⁵
1/0⁻⁴
PRESSURE (TORR.)